

Effective bias expansion for circumventing 21 cm foregrounds

Wenzer Qin ^{1, 2, 3} Kai-Feng Chen ^{1, 4} Katelin Schutz ⁵ and Adrian Liu ⁵

¹*Department of Physics, Massachusetts Institute of Technology, Cambridge, MA 02139, USA*

²*Center for Theoretical Physics, Massachusetts Institute of Technology, Cambridge, Massachusetts 02139, USA*

³*Center for Cosmology and Particle Physics, Department of Physics,
New York University, New York, NY 10003, USA*

⁴*MIT Kavli Institute, Massachusetts Institute of Technology, Cambridge, MA 02139, USA*

⁵*Department of Physics & Trottier Space Institute,
McGill University, Montréal, QC H3A 2T8, Canada*

The 21 cm line of neutral hydrogen is a promising probe of the Epoch of Reionization (EoR) but suffers from contamination by spectrally smooth foregrounds, which obscure the large-scale signal along the line of sight. We explore the possibility of indirectly extracting the 21 cm signal in the presence of foregrounds by taking advantage of nonlinear couplings between large and small scales, both at the level of the density field and a biased tracer of that field. When combined with effective field theory techniques, bias expansions allow for a systematic treatment of nonlinear mode-couplings in the map between the underlying density field and the 21 cm field. We apply an effective bias expansion to density information generated with `21cmFAST` using a variety of assumptions about which information can be recovered by different surveys and density estimation techniques. We find that the 21 cm signal produced by our effective bias expansion, combined with our least optimistic foreground assumptions, produces $\sim 30\%$ cross-correlations with the true 21 cm field. Providing complementary density information from high-redshift galaxy surveys yields a cross-correlation of 50–70%. The techniques presented here may be combined with foreground mitigation strategies in order to improve the recovery of the large-scale 21 cm signal.

I. INTRODUCTION

The time from the birth of the first stars to the end of the Epoch of Reionization (EoR) marks an important era for the astrophysics of galaxy formation and assembly, as well as for the underlying growth of cosmological structure [1–6]. The redshifted 21 cm line from neutral hydrogen is a direct probe of this period of cosmic time [7, 8], which is being actively targeted by many existing and proposed radio observatories [9–21]. In particular, radio interferometers have already set stringent upper bounds on the 21 cm power spectrum [20, 22–42], which have been used to constrain the properties of the intergalactic medium (IGM) at high redshifts [37, 42–44].

A major ongoing issue in 21 cm cosmology is that the signal is highly contaminated by foreground emission that is many orders of magnitude brighter (see Ref. [45] for a review). These foregrounds, which include Galactic synchrotron radiation, are expected to be spectrally smooth and will therefore affect large-scale modes of the 21 cm signal along the line of sight. Additionally, the chromatic response of interferometers can cause the foregrounds to contaminate other Fourier modes. Decomposing each wavevector into $\mathbf{k} \equiv (\mathbf{k}_\perp, k_\parallel)$, where k_\parallel denotes the Fourier modes parallel to the line of sight and \mathbf{k}_\perp represents the Fourier modes in the plane perpendicular to the line of sight, then in k_\perp - k_\parallel space, the region where foreground contamination occurs is referred to as the “foreground wedge” due to its shape [46–52].

It is difficult to completely subtract foregrounds [46, 53–58] in the wedge due to uncertainties in modeling both the foreground emission and the chromatic response of the instrument [25, 59–76]. Therefore, these modes are

often discarded, with many analyses of 21 cm data focusing on evading foreground-contaminated modes [77–81]. This effectively renders a large number of cosmological modes inaccessible to current experiments, significantly reducing their sensitivity. It also limits the possibility of correlating the 21 cm signal with complementary tracers of the matter field from high-redshift galaxy surveys or line intensity mapping experiments [82–84].

As with any biased tracer of the matter field, there is non-linear mode-coupling between large-scale and small-scale modes of the 21 cm field. In principle, it is therefore possible to take advantage of this mode-coupling to reconstruct large-scale information from uncontaminated measurements of small-scale modes. This type of reconstruction has been studied in the context of matter density and halo fields [85–87], as well as in 21 cm cosmology [88–90], although usually at low redshifts of $z \lesssim 5$. Past studies have also applied machine learning methods to reconstruct the foreground-obscured 21 cm modes [91–94]. On length scales where 21 cm fluctuations are only *mildly* nonlinear, one can use techniques inspired by effective field theory (EFT) to systematically treat these nonlinearities [95, 96]. For instance, it was recently shown that EFT methods applied to small-volume (high- k) hydrodynamical simulations of the 21 cm field can accurately predict larger volumes [97].

In this work, we further explore the predictive power that comes from the coupling between modes with different Fourier shapes in order to see how well we can recover foreground-obscured 21 cm modes. To test the robustness of the techniques used here, we make several different assumptions about which 21 cm modes are contaminated by foregrounds and what underlying den-

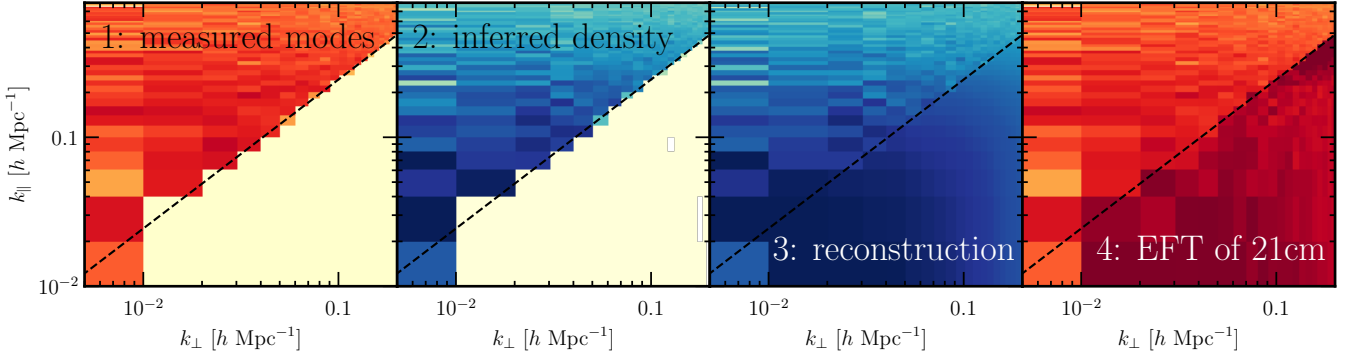


FIG. 1. The steps involved in our procedure. Starting at the left, radio telescopes will measure high- k 21 cm modes (*step 1*). Since the 21 cm signal is a biased matter tracer, one can infer the underlying matter density field information, which will also mostly be at high k_{\parallel} values (*step 2*). We can then take advantage of nonlinear couplings to reconstruct the missing density modes (*step 3*) and then use the bias expansion to translate the density fluctuations back into 21 cm fluctuations (*step 4*).

sity information is available. We also assess the impact of supplemental density information inferred from other probes in different parts of Fourier space, such as galaxy surveys, e.g. by the Nancy Grace Roman Space Telescope [98].

The rest of this paper is organized as follows. In Section II, we provide a conceptual overview of how we reconstruct missing modes and describe the various assumptions we make about what density information is available. In Section III, we briefly review the effective 21 cm bias expansion of Refs. [95, 96] and describe our methods for reconstructing missing density modes. In Section V, we present the results of applying the bias expansion to different combinations of density information, and also demonstrate the complementarity of measurements from galaxy surveys. We conclude in Section VI. Throughout this article, we use cosmological parameters from *Planck* 2018 [99].

II. CONCEPTUAL OVERVIEW

The pipeline for recovering the foreground-contaminated 21 cm signal, as schematically illustrated in Fig. 1, consists of four main steps:

1. Experiments such as HERA will measure the 21 cm signal outside of the foreground wedge.
2. From these 21 cm measurements, one can extract density information outside of the foreground wedge. With this density information and the 21 cm modes from step 1, one can infer the bias parameters describing their connection.
3. One can then reconstruct the density modes *inside* the foreground region by taking advantage of nonlinear mode-coupling in the matter density field.
4. Finally, with the bias parameters and linear density field, it is possible to map the density field back to

21 cm field using an effective bias expansion, thus obtaining 21 cm modes within foregrounds. We compare the predicted 21 cm modes to signals generated with *21cmFAST* to validate this approach.

While the first step poses a challenging data analysis problem, the second step in this pipeline is highly non-trivial from a theoretical perspective. In principle, since the 21 cm radiation is a biased tracer of the density field, one should be able to express the 21 cm field in terms of an expansion in powers of the density field, described in Section III A. This expansion could then be inverted in order to obtain the density fluctuations from the 21 cm fluctuations. However, in practice, nonlinear contributions make the information relatively difficult to extract [100]. These challenges have been extensively studied in the context of galaxy surveys, particularly for the purpose of reconstructing the linear density field and baryon acoustic oscillations [86, 87, 101–113], and some limited progress has been made based on using 21 cm information as a starting point [90, 114, 115].

Devising an optimal strategy for extracting density information from 21 cm fluctuations would be worth its own dedicated study, and therefore we choose to focus primarily on steps 3 and 4 in this work. However, we note that Ref. [116] has shown that step 2 is possible by adopting a gradient-based sampler to simultaneously infer the bias parameters and the underlying density field from the observed 21 cm modes outside the foreground wedge. Specifically, deep in the perturbative regime, the 21 cm field and density field are primarily related through the linear bias term which is local [96, 97]. This indicates that the density modes that can be recovered correspond to the same modes where one has uncontaminated 21 cm information. This is corroborated by the findings of Ref. [116], which showed explicitly that density modes outside the foreground wedge can be reliably inferred with up to 90% accuracy on large scales (depending on the region of Fourier space) assuming a $\sim 3\sigma$ detection of those same individual 21 cm modes. As it turns

out, the same approach of Ref. [116] can also be used to reconstruct some of the large-scale density modes in the foreground wedge because their forward model includes nonlinear mode-coupling. These results and future improvements to step 2 can interface with the framework presented here in a straightforward way.

Motivated by uncertainties about which modes can be reliably inferred, as this is an active line of inquiry, we consider multiple representative scenarios in the following discussion. Starting from the least optimistic case and moving to more ambitious possibilities, we assume that the density modes initially recovered are:

- the Fourier modes \mathbf{k} outside of the foreground wedge, which are those with [81]

$$|k_{\parallel}| \leq \frac{D_c(z)H(z)}{c(1+z)} |k_{\perp}|, \quad (1)$$

where $D_c(z)$ is the co-moving line-of-sight distance to redshift z [117], $H(z)$ is the Hubble parameter as a function of redshift, and c is the speed of light. We will refer to this as the “wedge” case and it corresponds to the most likely future scenario.

- the modes $k_{\parallel} > k_{\text{cut}}$, corresponding to a scenario where densely spaced or specifically arranged interferometer array configurations make it possible to use foreground mitigation strategies that may be able to recover wedge modes at high k_{\perp} [118, 119]. We also include this case since in our discussion because it enables a more direct comparison with results from the literature [90]. We will refer to this as the “flat” case.
- the modes $k > k_{\text{cut}}$, which has been used in the literature to approximate the limitations of galaxy surveys [90]. We also include this case as further motivation for studies of 21 cm foreground mitigation, to show how much more of the missing modes we can recover given additional small scale information. We will refer to this as the “isotropic” case.

We treat all three of these cases the same way in steps 3 and 4, with the only difference being the availability of modes entering into the reconstruction.

III. NONLINEAR MODE-COUPING AND RECONSTRUCTION

A. An effective bias expansion of the 21 cm signal

Here, we briefly review how one can predict the large-scale 21 cm signal from the underlying density field by applying the effective bias expansion described in Refs. [95, 96], which corresponds to the last step in Fig. 1.

In linear perturbation theory, density perturbations independently evolve with scale factor a as $\delta^{(1)} \sim D(a)$,

regardless of the length scale. Here $D(a)$ is the linear growth factor, corresponding to $D(a) \sim a$ in a matter-dominated universe. However, as structure formation progresses, nonlinear contributions increasingly couple different Fourier modes. We define k_{NL} as the wavenumber at which nonlinear contributions become significant, i.e. $k < k_{\text{NL}}$ or length scales greater than $\sim 1/k_{\text{NL}}$ can be treated perturbatively. In standard perturbation theory, the nonlinear evolution of δ is parameterized as an order-by-order expansion. Using bold subscripts to denote Fourier-transformed quantities, e.g. $(\delta)_{\mathbf{k}} \equiv \int d^3\mathbf{x} \delta(\mathbf{x}) e^{-i\mathbf{k}\cdot\mathbf{x}}$, this expansion is given by

$$\delta_{\mathbf{k}} = \sum_{n=1}^{\infty} a^n \delta_{\mathbf{k}}^{(n)}, \quad (2)$$

where the higher-order terms are in turn parameterized as convolutions of the linear density field,

$$\delta_{\mathbf{k}}^{(n)} = \int d^3\mathbf{q}_1 \cdots \int d^3\mathbf{q}_n (2\pi)^3 \delta^D \left(\mathbf{k} - \sum_{i=1}^n \mathbf{q}_i \right) \times F_n(\mathbf{q}_1, \dots, \mathbf{q}_n) \delta_{\mathbf{q}_1}^{(1)} \cdots \delta_{\mathbf{q}_n}^{(1)}, \quad (3)$$

where $d^3\mathbf{q}$ is shorthand for $d^3\mathbf{q}/(2\pi)^3$. The Dirac delta function δ^D enforces a relationship between the coupled modes that enter into the convolution kernels F_n , which have well-known recursion relations [120–122].

The matter velocity field \mathbf{v} can be decomposed into its divergence, $\theta = \nabla \cdot \mathbf{v}$, and curl, $\omega = \nabla \times \mathbf{v}$. The curl component decays like $\omega \sim 1/a$ in standard perturbation theory, so we neglect it. Meanwhile, in linear perturbation theory $\theta^{(1)} \sim \delta^{(1)}$. The divergence of the velocity field can then be expressed as an expansion similar to the density field,

$$\theta_{\mathbf{k}} = aH \sum_{n=1}^{\infty} a^n \theta_{\mathbf{k}}^{(n)}, \quad (4)$$

where higher-order terms are again expressed as convolutions of the linear density field,

$$\theta_{\mathbf{k}}^{(n)} = \int d^3q_1 \cdots \int d^3q_n (2\pi)^3 \delta^D \left(\mathbf{k} - \sum_{i=1}^n \mathbf{q}_i \right) \times G_n(\mathbf{q}_1, \dots, \mathbf{q}_n) \delta_{\mathbf{q}_1}^{(1)} \cdots \delta_{\mathbf{q}_n}^{(1)}, \quad (5)$$

and where the recursion relations for the G_n convolution kernels are also given in Refs. [120–122].

We then assume that fluctuations in the 21 cm intensity field, δ_{21} , trace the nonlinear matter density, and can thus be written as a local bias expansion in terms of δ . We include all operators respecting rotational and Galilean invariance up to second order in δ ,

$$(\delta_{21})_{\mathbf{k}} = b_1 \delta_{\mathbf{k}} - b_{\nabla^2} \left(\frac{k}{k_{\text{NL}}} \right)^2 \delta_{\mathbf{k}} + b_2 (\delta^2)_{\mathbf{k}} + b_{G2} (G_2)_{\mathbf{k}} + \cdots \quad (6)$$

The tidal (Galileon) operator is defined in configuration space as

$$\mathcal{G}_2 = (\nabla_i \nabla_j \phi)(\nabla^i \nabla^j \phi) - (\nabla^2 \phi)^2, \quad (7)$$

where ϕ is the gravitational potential. In addition to the linear and quadratic bias, the expansion in Eq. (6) includes b_{∇^2} , which captures local nonlinearities due to e.g. ionizing photons that travel long distances and is degenerate with leading-order EFT of LSS sound speed term [123]. We neglect the stochastic contribution to this expansion, as this term is negligible at the wavenumbers of interest [95].

The higher-order terms appearing in Eq. (6) involve integrating over nonlinear scales that are not well described using perturbative methods. For example, the term δ^2 which appears as a product in configuration space is written in Fourier space as a convolution,

$$(\delta^2)_k = \int d^3 q \delta_q \delta_{k-q}, \quad (8)$$

where the integration includes UV contributions from large wavenumbers (i.e. small length scales) which are beyond the regime of perturbative control. However, the long-wavelength modes that we are concerned with should be largely insensitive to small-scale nonlinear modes, and we thus add counterterms to each operator that cancel the UV-sensitive contributions up to a certain order in a procedure analogous to renormalization (see Refs. [124] and [96] for more details). For example, the first few terms of the renormalized δ^2 operator, which we denote as $[\delta^2]$, are given by

$$[\delta^2] = \delta^2 - \sigma^2(\Lambda) - \frac{68}{21} \sigma^2(\Lambda) \delta, \quad (9)$$

where Λ is the small-scale cutoff for the perturbative theory, $\sigma^2(\Lambda) = \int_0^\Lambda \frac{dq}{2\pi^2} q^2 P_L(q)$ is the variance in the linear matter fluctuations for $q < \Lambda$, and $P_L(q)$ is the linear matter power spectrum. The bias parameters must also shift to compensate for the newly added counterterms, and for a given parameter b_i , we write its renormalized counterpart as $b_i^{(R)}$.

Finally, we incorporate contributions from redshift space distortions (RSDs). Due to the peculiar velocities of 21 cm sources, \mathbf{v}_{pec} , the inferred coordinate of a source \mathbf{x}_r is related to its true coordinate \mathbf{x} by

$$\mathbf{x}_r = \mathbf{x} + \frac{\hat{\mathbf{n}} \cdot \mathbf{v}_{\text{pec}}}{aH} \hat{\mathbf{n}}, \quad (10)$$

where $\hat{\mathbf{n}}$ is the line-of-sight direction, a is the scale factor, and H is the Hubble parameter. One can then express the density field in redshift space in terms of the real-

space density using Eq. (10) and obtain

$$\begin{aligned} (\delta_r)_k = & \delta_k - i \frac{k_\parallel}{aH} (v_\parallel)_k - i \frac{k_\parallel}{aH} (\delta v_\parallel)_k \\ & - \frac{1}{2} \left(\frac{k_\parallel}{aH} \right)^2 (v_\parallel^2)_k - \frac{1}{2} \left(\frac{k_\parallel}{aH} \right)^2 (\delta v_\parallel^2)_k \\ & + \frac{i}{6} \left(\frac{k_\parallel}{aH} \right)^3 (v_\parallel^3)_k + \dots, \end{aligned} \quad (11)$$

where we have defined $v_\parallel = \hat{\mathbf{n}} \cdot \mathbf{v}_{\text{pec}}$ and $k_\parallel = \hat{\mathbf{n}} \cdot \mathbf{k}$, and Taylor expanded the expression by treating $k_\parallel v_\parallel/aH$ as a small number. This expansion is justified since, on the length scales that we are interested in, the peculiar velocities of sources are a small effect compared to the Hubble flow. The velocity fields can be calculated from the linear density field using Eqs. (4) and (5). This RSD expansion then contains new operators such as v_\parallel^2 which must also be renormalized.

Combining Eqs. (6) and (11) and renormalizing all UV-sensitive operators, the relationship between the 21 cm field and linear density field is thus given by

$$\begin{aligned} (\delta_{21,r})_k = & b_1^{(R)} \delta_k - b_{\nabla^2} k^2 \delta_k + b_2^{(R)} [\delta^2]_k + b_{G2}^{(R)} (\mathcal{G}_2)_k \\ & - i \frac{k_\parallel}{aH} [(v_\parallel)_k + b_1 (\delta v_\parallel)_k - b_{\nabla^2} k^2 (\delta v_\parallel)_k] \\ & - \frac{1}{2} \left(\frac{k_\parallel}{aH} \right)^2 [v_\parallel^2]_k + \dots \end{aligned} \quad (12)$$

This model has been shown to reproduce the 21 cm power spectrum from hydrodynamical simulations with errors at the percent level, and the field-level signal with errors at the $\mathcal{O}(10\%)$ level [96].

Since, throughout the text, we assume that both density and 21 cm measurements are available outside of some “wedge”-shaped, “flat”, or “isotropic” region, we fit the renormalized bias coefficients using Eq. (12) only over the available wavenumbers in each scenario. We perform a field-level fit for the coefficients by minimizing the function

$$\mathcal{A} = \sum_k \frac{|(\delta_{\text{sim}})_k - (\delta_{\text{EFT}})_k|^2}{V}, \quad (13)$$

where δ_{sim} is the 21 cm fluctuations generated from e.g. 21cmFAST, δ_{EFT} is the 21 cm signal predicted from the underlying density field using e.g. Eq. (12), and V is the volume of the simulation [96].

B. Reconstruction of missing density modes

For step 3 in Fig. 1, we use the procedure from Ref. [90] as one example for reconstructing missing modes at the level of the density field. Here, we summarize the main steps for constructing the estimator; more details about how to derive the following expressions can be found in Ref. [90].

In linear perturbation theory, different modes of an initially Gaussian density field evolve independently of one another; however, nonlinear gravitational evolution couples modes at different length scales. For example, the nonlinear density field can be written in terms of the linear matter overdensity $\delta^{(1)}$ as

$$(\delta_{\text{NL}})_{\mathbf{k}} = \delta_{\mathbf{k}}^{(1)} + \sum_{\alpha} \int d^3 \mathbf{q} F_{\alpha}(\mathbf{q}, \mathbf{k} - \mathbf{q}) \delta_{\mathbf{q}}^{(1)} \delta_{\mathbf{q}-\mathbf{k}}^{(1)} + \dots, \quad (14)$$

where α runs over distinct types of quadratic couplings and F_{α} represents the corresponding kernel. The kernels we examine in this study correspond to (1) the “growth” coupling, which can be thought of as the enhanced or suppressed growth of a small-scale mode due to being embedded in a larger-wavelength over/underdensity,

$$F_G(\mathbf{k}_1, \mathbf{k}_2) = \frac{17}{21}; \quad (15)$$

(2) the “shift” coupling, which can be thought of as the displacement of a mode due to the presence of another nearby over/underdensity,

$$F_S(\mathbf{k}_1, \mathbf{k}_2) = \frac{1}{2} \left(\frac{1}{k_1^2} + \frac{1}{k_2^2} \right) \mathbf{k}_1 \cdot \mathbf{k}_2; \quad (16)$$

and (3) the “tidal” coupling, which can be thought of as the tidal force on an overdensity/underdensity from being embedded in a varying gravitational field,

$$F_T(\mathbf{k}_1, \mathbf{k}_2) = \frac{2}{7} \left[\frac{(\mathbf{k}_1 \cdot \mathbf{k}_2)^2}{k_1^2 k_2^2} - \frac{1}{3} \right]. \quad (17)$$

At second order in standard perturbation theory, the kernel F_2 appearing in Eq. (3) is the sum of all three kernels listed above [121, 125]. These couplings also arise in configuration-space expansions describing biased tracers of matter. For example, a quadratic bias term δ^2 will have a kernel corresponding to the growth coupling. Similarly, the Fourier-transformed Galileon operator defined in Eq. (7) will have a kernel corresponding to the tidal coupling. Given density information in some part of Fourier space, we can use these mode couplings to reconstruct missing wavenumbers.

Given the nonlinear density field, the minimum variance unbiased estimator for the linear density field is given by [90]

$$\hat{\Delta}_{\alpha, \mathbf{K}} = N_{\alpha}(\mathbf{K}) \times \int d^3 \mathbf{q} \frac{f_{\alpha}(\mathbf{q}, \mathbf{K} - \mathbf{q})}{2P_{\text{NL}}(q)P_{\text{NL}}(|\mathbf{K} - \mathbf{q}|)} (\delta_{\text{NL}})_{\mathbf{q}} (\delta_{\text{NL}})_{\mathbf{K}-\mathbf{q}} \quad (18)$$

where the normalization factor is given by

$$N_{\alpha}(\mathbf{K}) = \left(\int d^3 \mathbf{q} \frac{f_{\alpha}(\mathbf{q}, \mathbf{K} - \mathbf{q})^2}{2P_{\text{NL}}(q)P_{\text{NL}}(|\mathbf{K} - \mathbf{q}|)} \right)^{-1} \quad (19)$$

and also represents noise on the estimator from cosmic variance and shot noise, f_{α} is related to the kernels described previously by

$$f_{\alpha}(\mathbf{q}_1, \mathbf{q}_2) = 2 [F_{\alpha}(\mathbf{q}_1 + \mathbf{q}_2, -\mathbf{q}_1) P_{\text{L}}(q_1) + (1 \leftrightarrow 2)], \quad (20)$$

$P_{\text{NL}}(q)$ is the nonlinear matter power spectrum, and $P_{\text{L}}(q)$ the linear power spectrum. The expression in Eq. (18) is derived assuming there is only a single mode-coupling, e.g. only one of the growth, shift, or tidal type couplings present. Other couplings not accounted for in the estimator become sources of noise or contamination; see Ref. [90] for details.

We have validated our calculation by checking that we can reproduce $N_{\alpha}(\mathbf{K})$ in Ref. [90] in the wavenumber range where our results overlap when we make the same assumptions. Moreover, in agreement with Ref. [90], we find that the growth-type coupling has the lowest noise of the three listed above. Therefore, for the rest of this work, we will use the growth coupling when including the step of density reconstruction.

In Ref. [90], the normalization for the estimator is derived by requiring that it be unbiased at the field level, e.g. the expectation value of the estimator is the true linear density field. As a result, the cross-spectrum of the estimator with $\delta^{(1)}$ is given by

$$\langle \delta_{\mathbf{k}}^{(1)} \hat{\Delta}_{\alpha, \mathbf{k}'} \rangle = (2\pi)^3 \delta(\mathbf{k} - \mathbf{k}') P_{\text{L}}(k). \quad (21)$$

This property is appropriate for applications such as cross-correlating the estimator with galaxy surveys. However, this also means that the auto-spectrum of the estimator is

$$\langle \hat{\Delta}_{\alpha, \mathbf{k}} \hat{\Delta}_{\alpha, \mathbf{k}'} \rangle = (2\pi)^3 \delta(\mathbf{k} - \mathbf{k}') N_{\alpha}(k). \quad (22)$$

In this work, since we are more concerned with the power spectrum of the estimator, we require that the estimator be unbiased at the level of the power spectrum. We accomplish this by replacing the normalization N_{α} in Eq. (18) and instead fixing the amplitude of each Fourier mode to its value inferred from the average power spectrum so that $|\hat{\Delta}_{\alpha, \mathbf{K}}|^2 = P_{\text{NL}}(k)$, which can be obtained from a cosmological Boltzmann code like CAMB [126] or CLASS [127]. While this procedure artificially suppresses cosmic variance, it ensures that we recover the correct matter power spectrum, and subsequently the correct 21 cm power spectrum after applying the bias expansion described in the previous Section.

Since the validity of the estimator in Eq. (18) relies on the linear and quadratic terms dominating Eq. (14), the field δ_{NL} must be smoothed using some window function $W(k)$ in order to exclude the high- k modes that are the most nonlinear. The estimator in Eq. (18) can then be written in terms of convolutions, and therefore calculated using the convolution theorem. For example, if we substitute Eq. (15) into Eq. (20) to obtain f_G and use this to calculate the estimator, then the integral in Eq. (18) can be written as a convolution over the fields

$$(\delta_A)_{\mathbf{k}} = \frac{(\delta_{\text{NL}}^W)_{\mathbf{k}}}{P_{\text{NL}}(k)}, \quad (\delta_B)_{\mathbf{k}} = \frac{(\delta_{\text{NL}}^W)_{\mathbf{k}} P_{\text{L}}(k)}{P_{\text{NL}}(k)}, \quad (23)$$

where δ_{NL}^W denotes the smoothed matter field. Hence, we can apply the inverse Fourier transformation to each of

these fields, multiply the configuration-space fields, and Fourier transform the result to obtain the estimator. For the shift and tidal kernels, which have somewhat more complicated expressions, one can expand Eq. (18) into a sum of many convolutions over quantities similar to those appearing in Eq. (23).

To summarize, we use the available density information (e.g. outside of foregrounds) to calculate the expressions in Eq. (23). From $(\delta_A)_k$ and $(\delta_B)_k$ we can then calculate $\hat{\Delta}_{\alpha,\mathbf{k}}$, which provides an estimate of the missing density information.

IV. SETUP AND MOCK FIELDS

In order to calculate the right-hand side of Eq. (12), one either needs knowledge of both the matter density field and velocity field, or the linear density field alone since it can be used to calculate the full density through Eq. (2) and the velocity through Eq. (4). In what follows, we assume that we only have information about the underlying density and not the velocity. Therefore, we must assume knowledge of the *linear* density field even if the output of step 2 includes nonlinear contributions (i.e. the full matter density field) in actuality. As we are primarily concerned with the mildly nonlinear regime, we expect any contamination from these spurious contributions to be small since it only appears at higher order.

In addition to the density information obtained under the foreground scenarios described in Section II, we demonstrate the impact of various assumptions about the linear density $\delta^{(1)}$:

- $\delta^{(1)} = \delta_{m,obs} \oplus 0^{FG}$: the matter density only outside of the foreground region, which we assume can be inferred from 21 cm measurements, per step 2 in Section II. In the absence of information about the density, we set $\delta^{(1)} = 0$ for modes inside the foreground-contaminated region before substituting into the effective bias expansion. This shows how well we can recover the 21 cm signal in the presence of foregrounds using *only* the bias expansion, in the absence of any density reconstruction. Fourier modes of δ_{21} within the foreground region only receive nonlinear contributions in this case due to their coupling to modes outside the region.
- $\delta^{(1)} = \delta_{m,obs} \oplus \delta_{m,recon}^{FG}$: the combination of $\delta_{m,obs}$ and density information inside the foreground region reconstructed using the method described in Section III B.
- $\delta^{(1)} = \delta_{m,obs} \oplus \delta_{m,gal}$: the combination of $\delta_{m,obs}$ from 21 cm observations and matter density fluctuations inferred from galaxy surveys, which we describe further in Sec. V B (including our assumptions about redshift uncertainties). For modes that are within the 21 cm foreground region and not covered by galaxy surveys, we again set $\delta^{(1)} = 0$.

Foregrounds	# modes	# perturbative
Full	2,406,104	41,851
Isotropic	2,403,899	39,646
Flat	2,100,852	18,362
Wedge	105,765	3,122

TABLE I. The number of modes available from the 21cmFAST box under each assumption about modes lost to foregrounds, as well as the number of perturbative modes ($k < k_{NL}$) in each case. The nonlinear scale k_{NL} and the foreground wedge are calculated at $z = 8.5$.

- $\delta^{(1)} = \delta_{m,full}$: the full matter density field, both inside and outside the foreground region. While this is an overly optimistic assumption, the purpose here is to show the most accurate 21 cm signal that could in principle be recovered using our perturbative methods.

The mock 21 cm brightness temperature fields that we compare our methods against are generated using 21cmFAST [128, 129], a semi-numerical modeling tool capable of efficiently producing realizations of the universe during the Cosmic Dawn and the EoR. 21cmFAST utilizes second-order Lagrangian perturbation theory (2LPT) to evolve the initial conditions of the universe to the desired redshift, and uses the excursion-set formalism [130] to generate the process of reionization. Such a formalism assumes that reionization is driven by galaxies and uses a set of empirical scaling relations to describe the astrophysical properties of these galaxies. In this work, we assume a saturated spin temperature and ignore the effect of X-ray heating. We adopt the astrophysical parametrization and fiducial parameters described in Ref. [131] to model reionization, which was shown to describe high-redshift galaxy luminosity functions well (up to $z \sim 10$). For the purpose of testing our reconstruction methods, we generate a $(500 \text{ cMpc})^3$ box on a 134^3 grid at a redshift of $z = 8.5$.

We use 21cmFAST because of its ability to quickly generate such large volumes, which is necessary for testing the reconstruction of large-scale modes. The methods studied in this work could also be tested against other analytic and semi-analytic methods that can generate large volumes, such as *Zeus21* [132]. In this work, we do not validate our method against hydrodynamical simulations, which in principle capture a richer description of the astrophysical complexities underlying reionization. However, if such large hydrodynamical simulations were available, we expect that our methods would also work well in that context, since the effective bias expansion is able to accurately describe nonlinear mode-coupling for the purpose of enlarging simulations [96, 97].

After generating the fields with 21cmFAST, we remove modes that we assume are contaminated by foregrounds using the cuts described in Section III B. For the “flat” and “isotropic” foregrounds, we use $k_{cut} = 0.15$

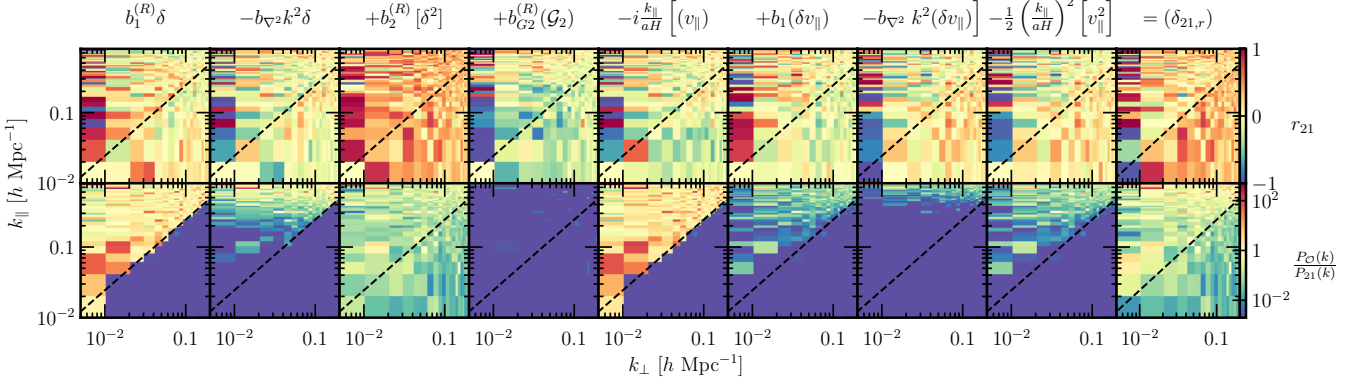


FIG. 2. Terms in the bias expansion when applied to the $\delta_{m,\text{obs}}$ with density modes missing in the foreground wedge. The first row shows the cross-correlation of each term with the true 21 cm signal, and the second row shows the ratio of the power spectrum of each term to the 21 cm power spectrum from 21cmFAST. Within the foreground region, the only term with a significant amplitude is the quadratic bias (δ^2), which shows a $\sim 30\%$ correlation with the 21 cm fluctuations and is the dominant contribution to the bias expansion.

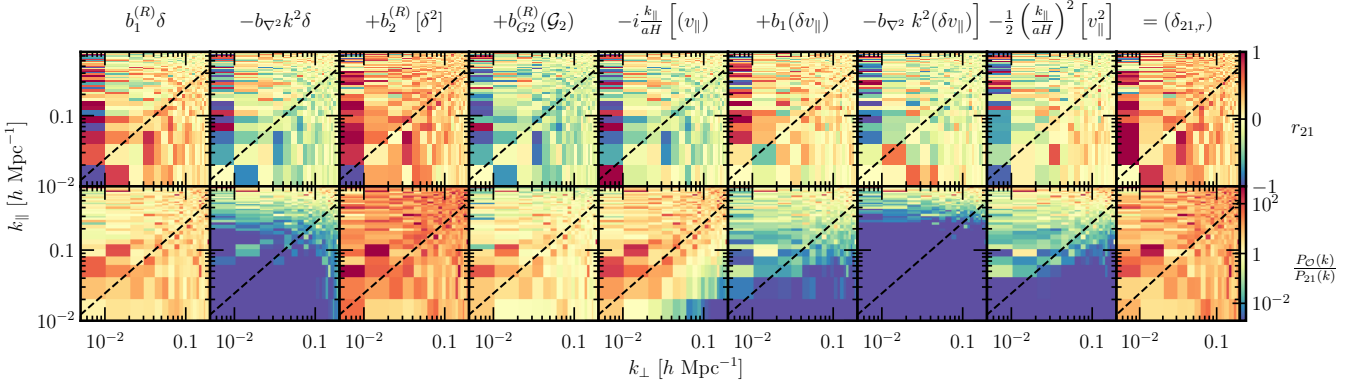


FIG. 3. Same as Fig. 2, but applying density reconstruction to obtain density modes within the foreground wedge before mapping to 21 cm with the bias expansion. Compared to Fig. 2, including density reconstruction improves the recovery of both the phase information and amplitude of the linear terms, δ and $k^2\delta$. Nonlinear terms such as δ^2 and \mathcal{G}_2 have an enhanced amplitude compared to Fig. 2. The sum of the terms, shown in the rightmost panel, has a similar cross-correlation to the true 21 cm signal as in Fig. 2, since the nonlinear terms already exhibited a significant cross-correlation.

Mpc^{-1} . The number of modes left uncontaminated by foregrounds is given in the second column of Table I; the maximum number of modes is $134^3 = 2,406,104$.

To evaluate the expression in Eq. (18), we first filter the nonlinear small scales from the tracer field. As above, we denote the smoothed tracer field by δ_{NL}^W . We calculate the wavenumber cutoff k_{NL} for this filter by smoothing δ_{NL} with a Gaussian window function on increasingly large length scales until the largest overdensity is less than 0.8; the value of k_{NL} is not particularly sensitive to the choice of value that we use for largest overdensity or the choice of window function [96]. For the 21cmFAST realization used in this work, we find that the nonlinear scale is approximately $k_{NL} = 0.4 \text{ cMpc}^{-1}$ at $z=8.5$. The third column of Table I shows the number of uncontaminated modes that are in the perturbative regime, i.e. with $k < k_{NL}$. To evaluate the total power spectra in Eq. (23), we

use the CAMB Boltzmann code [133].

V. RESULTS

In this Section, we apply the methods described in Section II to fields generated using 21cmFAST. We use two metrics for determining the success of recovering the 21 cm signal. The first is the cross-correlation between a field and the true 21 cm signal, which is given by

$$r_{21}(\mathbf{k}) = \frac{P_{X,21}(\mathbf{k})}{\sqrt{P_X(\mathbf{k})P_{21}(\mathbf{k})}}, \quad (24)$$

where X represents any field. Note from the normalization of this expression that r_{21} is insensitive to the amplitude of the field X and therefore only encodes information about how well the phase of each Fourier mode

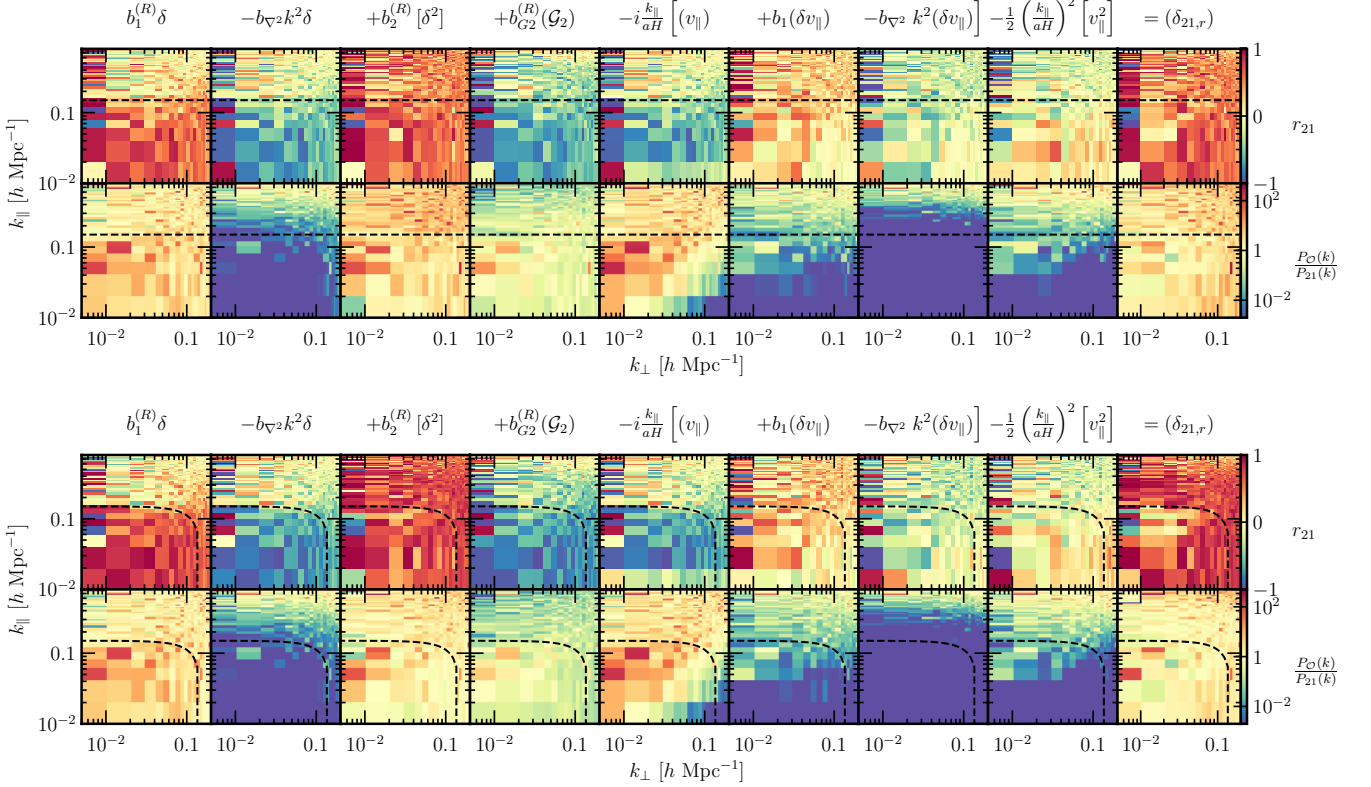


FIG. 4. Same as Fig. 3, but now assuming the flat (*top panel*) and isotropic (*bottom panel*) foreground shapes. Both cases show improved accuracy in the cross-correlation and power spectrum in foreground-contaminated regions as compared to the case with wedge-shaped foregrounds shown in Fig. 3.

in X matches the 21 cm field realization. To capture the amplitude information, we can instead look at the ratio of the power spectrum of the desired field, which does not contain phase information, to the power spectrum of the mock 21 cm signal, $P_X(\mathbf{k})/P_{21}(\mathbf{k})$.

A. Individual terms

We first compare individual terms in the bias expansion to the mock 21 cm signal to determine which terms hold the greatest importance for an accurate reconstruction. We compute both r_{21} and P_X/P_{21} for each of the eight individual terms appearing in Eq. (12), including the best-fit bias coefficients and any other prefactors that multiply the RSD terms. We can then compare these to the values of r_{21} and P_X/P_{21} obtained by taking the sum of all the terms in the bias expansion. Note that we take this sum before computing the power spectrum, since the power spectrum of a sum is not equal to the sum of individual power spectra.

Fig. 2 shows the result of applying the bias expansion assuming $\delta^{(1)} = \delta_{\text{m,obs}}$ outside of the foreground wedge and $\delta^{(1)} = 0$ inside the wedge, i.e. without performing any density reconstruction. The only terms that show any significant amount of cross-correlation with the true

21 cm field in the wedge are those corresponding to δ^2 and G_2 , with typical r_{21} values of 0.3 and -0.2 , respectively. Moreover, δ^2 is the only term with a large enough amplitude inside the wedge to contribute significantly to the overall bias expansion, with all other terms comprising sub-percent level contributions to the power spectrum in the foreground wedge. It is perhaps surprising that there is any appreciable level of correlation with the 21 cm field inside the wedge given that we are assuming that the initial linear density is identically zero in that region of Fourier space. Terms in Eq. (12) that are linear in $\delta^{(1)}$, which lack mode coupling, are therefore greatly suppressed relative to nonlinear terms such as δ^2 and G_2 , although we note that even $\delta = \delta^{(1)} + \delta^{(2)} + \dots$ has nonlinear contributions appearing in the linear bias. Nevertheless, these nonlinear terms by themselves do have some predictive power in the foreground wedge.

Applying the estimator described in Section III B to reconstruct density information within foregrounds (i.e. substituting $\delta_{\text{m,obs}} \oplus \delta_{\text{m,recon}}^{\text{FG}}$ into Eq. (12)), we obtain the term-by-term cross correlations and power spectra shown in Fig. 3. The linear terms in the expansion now show improved cross-correlation in the wedge at the level of about ± 0.2 , and also exhibit an increase in the amplitude of their power spectra. Fully nonlinear terms like δ^2 and G_2 show a similar level of cross-correlation as in Fig. 2;

however, their amplitude in the foreground wedge is now magnified, with P_{G_2} exceeding the true power spectrum by a factor of about 3.5 and P_{S^2} exceeding the true power spectrum by a factor of about 35. Although we see an improvement in the signal recovery on a term-by-term basis (particularly in the linear terms) once we include reconstructed density modes, we find that the improvement is less significant with all the terms summed together. This is because the most-improved terms are intrinsically less correlated to the true 21 cm field, and thus their better reconstruction does not significantly improve overall accuracy.

In Fig. 4, we perform a similar analysis assuming different foreground shapes prior to performing density reconstruction. In these cases, we see that the cross-correlation across the first several terms is higher than for the wedge-shaped foreground region: for the “flat” foregrounds, the first five terms all show cross-correlations of $|r_{21}| \sim 0.5\text{--}0.6$, and for the “isotropic” foregrounds, we see cross-correlations of $|r_{21}| \sim 0.6\text{--}0.7$. Since the “flat” and “isotropic” foreground shapes include more modes in the perturbative regime, compared to the wedge-shaped case (see again Table I), this leads to an improved reconstruction of modes within the foreground region, and therefore the cross-correlation for the linear terms is now comparable to that of the nonlinear terms. This is also evident in the fact that the “isotropic” scenario contains more perturbative modes than the “flat” case, and therefore shows improved cross-correlation over the flat foregrounds.

Summing all the individual terms to obtain the total 21 cm field, we find that the cross-correlation in the foreground region is higher than for the wedge-shaped foregrounds, and the recovered amplitude of the power spectrum is closer to that of the 21cmFAST power spectrum. While the recovered power spectrum in the presence of wedge-shaped foregrounds is too large by a factor of about 23, this improves to only a factor of 6.4 for flat-shaped foregrounds and 4.0 for isotropic foregrounds. This improvement can again be attributed to the fact that these foreground shapes mean that our procedure starts with more perturbative modes, and thus we have better information with which to accurately reconstruct the amplitude of modes in the foreground region, as well as calculate the contribution of nonlinear terms.

B. Adding density information from galaxy surveys

Galaxies are a biased tracer of the underlying matter density, and a large number of galaxies present during the EoR will soon be observed thanks to ground and space-based surveys [134–138]. However, the density field inferred from galaxies is only accurate for wavenumbers less than some value of k_{\parallel} , as uncertainties in the measured redshifts of the observed galaxies σ_z translate to uncertainties in their line-of-sight distances. Here, we assume a galaxy survey can measure the density field below $k_{\parallel} \leq H(z)/c/\sigma_z$ [82]. We note that as galaxy surveys

have high angular resolution, this k_{\parallel} threshold is constant across k_{\perp} . Typically, photometric redshift uncertainties are around $\sigma_z \sim 0.5$ [134, 139] for dropout galaxies and $\sigma_z \sim 0.1$ for galaxies selected with a narrow-band filter [140, 141]. With follow-up observations by spectroscopic instruments, these measurements can be significantly improved with uncertainties as low as e.g. $\sigma_z \sim 0.001$ for the grism spectroscopy that will be available for the High-Latitude Wide Area Survey from the Nancy Grace Roman Space Telescope [98, 142]. In this discussion, we will be conservative by assuming a relatively large redshift uncertainty of $\sigma_z \sim 0.05$, with the understanding that improvements to this will only increase the level of signal recovery. This redshift uncertainty corresponds to measuring $k_{\parallel} < 0.11h \text{ Mpc}^{-1}$ in the density field.

In Fig. 5, we show r_{21} and P_{total}/P_{21} for the 21 cm signal calculated assuming wedge-shaped foregrounds using different assumptions about the underlying density field. In order to ensure that differences between each column are not merely due to changes in the best-fit bias parameters, in each panel we use the same bias parameters as determined from the full density field. The first column shows the result of substituting the full density field, $\delta_{m,\text{full}}$, into Eq. (12). This is the best recovery of the 21 cm signal that we could ever obtain using the bias expansion. Here, we see that the cross-correlation is about 0.9 for wavenumbers within the perturbative regime. The amplitude of the power spectrum is also recovered with high accuracy and is within a factor of 1.5 of the true 21 cm power spectrum.

The middle two columns serve as a comparison of the total reconstructed 21 cm field in the wedge with and without performing density reconstruction in the wedge. Hence, they are quite similar to the final columns of Figs. 2 and Figs. 3, but as explained above are constructed using a slightly different set of bias parameters. As discussed in Section V A, the cross-correlation is slightly better *without* first performing density reconstruction. In other words, even if we assume that the matter density in the foreground wedge is *zero*, which is clearly incorrect, the mode-coupling intrinsic to the EFT terms is enough to yield a cross-correlation at the level of $r \sim 0.3$. This behavior can be understood as arising from the relative contribution of the linear terms with and without in-wedge density reconstruction, as described in Section V A: the slight degradation of the cross-correlation is due to the fact that the linear terms in the bias expansion are less correlated with the true 21 cm fluctuations than the nonlinear terms. Additionally, without first performing density reconstruction, the reconstructed in-wedge 21 cm field underestimates the power spectrum by a factor of 8, due to the fact that we are missing contributions to the 21 cm fluctuations from many of the underlying density modes, whereas with density reconstruction the reconstructed 21 cm field overestimates the power spectrum by a factor of 90 (this is larger than what was reported in the previous section due to the different bias coefficients).

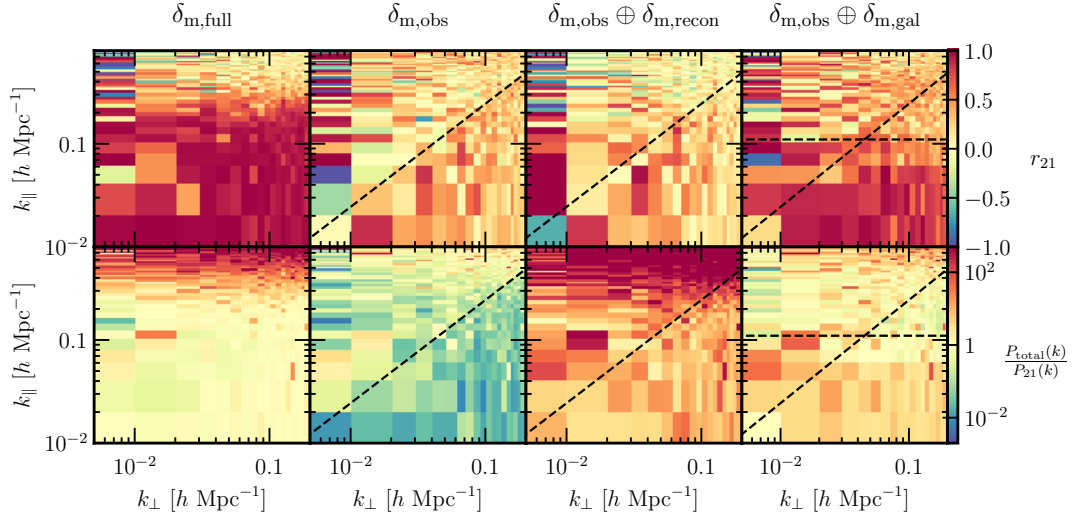


FIG. 5. The 21 cm signal resulting from substituting the density field with different modifications into Eq. 12. The first row shows the cross-correlation with the true 21 cm signal, r_{21} , and the second row shows the ratio of the power spectra of the two fields. For the last three columns, we assume $\delta_{m,\text{obs}}$ are the density modes lying outside of a wedge-shaped foreground region. In order to facilitate comparison of the different input density fields, we use the bias coefficients fit using the full density field across all columns.

The last column of Fig. 5 shows the result of substituting $\delta_{m,\text{obs}} \oplus \delta_{m,\text{Roman}}$ into Eq. (12). In this case, for modes that are within the foreground wedge and also not covered by the galaxy survey, the recovered cross-correlation is at the level of 0.5, and the power spectrum is within a factor of a few of the true amplitude. This is a clear improvement over using either $\delta_{m,\text{obs}}$ or $\delta_{m,\text{obs}} \oplus \delta_{m,\text{recon}}$. This highlights the complementarity of high redshift galaxy surveys to 21cm experiments, and motivates their joint use in recovering the underlying density field as well as reconstruction of 21 cm modes obscured by foregrounds.

VI. CONCLUSION

Separating the information in long-wavelength modes along the line of sight from foregrounds is a longstanding problem of 21 cm cosmology. Bias expansions provide a map between density fluctuations and tracers such as 21 cm fluctuations, and may thus be used to indirectly recover 21 cm information within foregrounds. In this work, we have tested how well one can reconstruct the 21 cm fluctuations using the bias expansion under different scenarios about the available density information.

Assuming that we have a method of obtaining density information outside of the foreground wedge [116], we find that simply applying our bias expansion to these modes already yields $\sim 30\%$ cross-correlations with the true 21 cm signal within the foreground region, due to non-linear couplings between small- and large-scale modes. Applying the density reconstruction method of Ref. [90] to obtain additional density information *within*

the foreground wedge improves the recovery of linear contributions to the 21 cm signal within the foreground region. For the wedge-shaped foreground scenario, density reconstruction does not improve the overall cross-correlation. Density reconstruction applied to the “flat” and “isotropic” scenarios yields results that are much improved compared to the density-reconstructed “wedge” case, giving cross-correlations as high as 70% and power spectra that are within a factor of a few of the true value—this motivates further study of independent methods for extracting small-scale density information.

For comparison, we also study the impact of including density information from galaxy surveys. This information is very complementary, as galaxy surveys tend to be sensitive to low values of k_{\parallel} less than some value corresponding to redshift uncertainties, which are the most contaminated modes in 21 cm observations. We find that with the inclusion of galaxy survey information, the cross-correlation of recovered 21 cm modes with the true 21 cm signal can be as high as 50% even for our least optimistic foreground assumptions.

From an information theory point of view, the reconstructed large-scale 21 cm modes do not add additional information at the field level, as they are determined solely from the small-scale modes. However, our results nonetheless demonstrate that the EFT is capable of capturing mode couplings generated by astrophysics-driven modeling frameworks such as 21cmFAST. Moreover, these reconstructed large-scale modes enable straightforward cross-correlation with other large-scale probes such as galaxy surveys without resorting to higher-order statistics such as the bispectrum. Our method also provides a potential route to create large-scale 21 cm templates at

the field level to uncover foreground-contaminated modes in the data through a matched-filter approach [58].

We emphasize that the methods presented here can build upon density reconstruction methods such as those presented in Ref. [90], but are conceptually different. While that work used measurements of biased tracers to reconstruct the matter density on scales obscured by foregrounds, the present work is concerned with whether one can use information about the density in small scales to obtain the 21 cm modes obscured by foregrounds. In this work, we have only explored the interface of the two methods by using the density estimator of Ref. [90] to supplement the small-scale density information assumed here. However, it may be instructive in the future to explore other ways in which these methods complement each other.

In summary, we have demonstrated that bias expansions combined with EFT-based treatments of nonlinear mode-coupling provide a useful starting point for recovering 21 cm information lost to foregrounds. Their utility is enhanced when combined with reliable extractions of the underlying density field within the foreground region, e.g. from galaxy surveys. There are a number of potential directions for improvement on the results presented here. For example, the density estimator of Ref. [90] that we apply throughout is derived using an unrenormalized bias expansion; it would be instructive to rederive this estimator using renormalized operators and including all of the appropriate counterterms. Moreover, an assumption that we make throughout this work is that one can extract density information outside of the 21 cm foreground

wedge from 21 cm measurements due to the strength of the linear bias term. However, this assumption merits a detailed study in its own right and new techniques to extract this density information, such as those presented in Ref. [116], could be combined with the techniques studied here in a straightforward way. We leave these as directions for future study.

ACKNOWLEDGMENTS

It is a pleasure to thank Simon Foreman and Julian Muñoz for helpful discussions and comments on this paper. W.Q. was supported by the National Science Foundation Graduate Research Fellowship under Grant No. 2141064 and a grant from the Simons Foundation (Grant Number SFI-MPS-SFJ-00006250, W.Q.). K.-F.C. acknowledges support from the Mitacs Globalink Research Award, Taiwan Think Global Education Trust Scholarship, and the Taiwan Ministry of Education’s Government Scholarship to Study Abroad. K.S. acknowledges support from a Natural Sciences and Engineering Research Council of Canada (NSERC) Subatomic Physics Discovery Grant and from the Canada Research Chairs program. A.L. acknowledges support from an NSERC Discovery Grant and a Discovery Launch Supplement, and the William Dawson Scholarship at McGill. This analysis made use of Numpy [143], Scipy [144], Jupyter [145], tqdm [146], and Matplotlib [147].

-
- [1] Abraham Loeb and Rennan Barkana, “The Reionization of the Universe by the First Stars and Quasars,” *ARA&A* **39**, 19–66 (2001), arXiv:astro-ph/0010467 [astro-ph].
 - [2] Saleem Zaroubi, “The Epoch of Reionization,” in *The First Galaxies*, Astrophysics and Space Science Library, Vol. 396, edited by Tommy Wiklund, Bahram Mobasher, and Volker Bromm (2013) p. 45, arXiv:1206.0267 [astro-ph.CO].
 - [3] Brant E. Robertson, “Galaxy Formation and Reionization: Key Unknowns and Expected Breakthroughs by the James Webb Space Telescope,” *ARA&A* **60**, 121–158 (2022), arXiv:2110.13160 [astro-ph.CO].
 - [4] Matthew McQuinn, Adam Lidz, Oliver Zahn, Suvendra Dutta, Lars Hernquist, and Matias Zaldarriaga, “The Morphology of HII Regions during Reionization,” *Mon. Not. Roy. Astron. Soc.* **377**, 1043–1063 (2007), arXiv:astro-ph/0610094.
 - [5] Andrei Mesinger, “Understanding the Epoch of Cosmic Reionization,” *Underst. Epoch Cosm. Reionization Challenges Prog.* **423** (2016), 10.1007/978-3-319-21957-8.
 - [6] Adrian Liu, Jonathan R. Pritchard, Rupert Allison, Aaron R. Parsons, Uroš Seljak, and Blake D. Sherwin, “Eliminating the optical depth nuisance from the CMB with 21 cm cosmology,” *Phys. Rev. D* **93**, 043013 (2016), arXiv:1509.08463 [astro-ph.CO].
 - [7] Steven Furlanetto, S. Peng Oh, and Frank Briggs, “Cosmology at Low Frequencies: The 21 cm Transition and the High-Redshift Universe,” *Phys. Rept.* **433**, 181–301 (2006), arXiv:astro-ph/0608032.
 - [8] Jonathan R. Pritchard and Abraham Loeb, “21 cm cosmology in the 21st century,” *Reports on Progress in Physics* **75**, 086901 (2012), arXiv:1109.6012 [astro-ph.CO].
 - [9] Raul A. Monsalve, Alan E. E. Rogers, Judd D. Bowman, and Thomas J. Mozdzen, “Calibration of the EDGES High-band Receiver to Observe the Global 21 cm Signature from the Epoch of Reionization,” *ApJ* **835**, 49 (2017), arXiv:1602.08065 [astro-ph.IM].
 - [10] Jishnu Nambissan T., Ravi Subrahmanyam, R. Somashekar, N. Udaya Shankar, Saurabh Singh, A. Raghunathan, B. S. Girish, K. S. Srivani, and Mayuri Sathyaranayana Rao, “SARAS 3 CD/EoR Radiometer: Design and Performance of the Receiver,” *arXiv e-prints* , arXiv:2104.01756 (2021), arXiv:2104.01756 [astro-ph.IM].
 - [11] L. Philip, Z. Abdurashidova, H. C. Chiang, N. Ghazi, A. Gumba, H. M. Heilgendorff, J. M. Jáuregui-García, K. Malepe, C. D. Nunhokee, J. Peterson, J. L. Sievers, V. Simes, and R. Spann, “Probing Radio Intensity at High-Z from Marion: 2017 Instrument,” *Jour-*

- nal of Astronomical Instrumentation **8**, 1950004 (2019), arXiv:1806.09531 [astro-ph.IM].
- [12] Aaron R. Parsons, Donald C. Backer, Griffin S. Foster, Melvyn C. H. Wright, Richard F. Bradley, Nicole E. Gugliucci, Chaitali R. Parashare, Erin E. Benoit, James E. Aguirre, Daniel C. Jacobs, Chris L. Carilli, David Herne, Mervyn J. Lynch, Jason R. Manley, and Daniel J. Werthimer, “The Precision Array for Probing the Epoch of Re-ionization: Eight Station Results,” *AJ* **139**, 1468–1480 (2010), arXiv:0904.2334 [astro-ph.CO].
- [13] M. P. van Haarlem, M. W. Wise, A. W. Gunst, G. Heald, J. P. McKean, J. W. T. Hessels, A. G. de Bruyn, R. Nijboer, J. Swinbank, R. Fallows, M. Brentjens, A. Nelles, R. Beck, H. Falcke, R. Fender, J. Hörandel, L. V. E. Koopmans, G. Mann, G. Miley, H. Röttgering, B. W. Stappers, R. A. M. J. Wijers, S. Zaroubi, M. van den Akker, A. Alexov, J. Anderson, K. Anderson, A. van Ardenne, M. Arts, A. Asgekar, I. M. Avruch, F. Batejat, L. Bähren, M. E. Bell, M. R. Bell, I. van Bemmel, P. Bennema, M. J. Bentum, G. Bernardi, P. Best, L. Bîrzan, A. Bonafede, A. J. Boonstra, R. Braun, J. Bregman, F. Breitling, R. H. van de Brink, J. Broderick, P. C. Broekema, W. N. Brouw, M. Brüggen, H. R. Butcher, W. van Capellen, B. Ciardi, T. Coenen, J. Conway, A. Coolen, A. Corstanje, S. Damstra, O. Davies, A. T. Deller, R. J. Dettmar, G. van Diepen, K. Dijkstra, P. Donker, A. Doorduin, J. Dromer, M. Drost, A. van Duin, J. Eisloffel, J. van Enst, C. Ferrari, W. Frieswijk, H. Gankema, M. A. Garrett, F. de Gasperin, M. Gerbers, E. de Geus, J. M. Grießmeier, T. Grit, P. Gruppen, J. P. Hamaker, T. Hassall, M. Hoeft, H. A. Holties, A. Horneffer, A. van der Horst, A. van Houwelingen, A. Huijgen, M. Iacobelli, H. Intema, N. Jackson, V. Jelic, A. de Jong, E. Juette, D. Kant, A. Karastergiou, A. Koers, H. Kollen, V. I. Kondratiev, E. Kooistra, Y. Koopman, A. Koster, M. Kuniyoshi, M. Kramer, G. Kuper, P. Lambopoulos, C. Law, J. van Leeuwen, J. Lemaitre, M. Loose, P. Maat, G. Macario, S. Markoff, J. Masters, R. A. McFadden, D. McKay-Bukowski, H. Meijering, H. Meulman, M. Mevius, E. Middelberg, R. Millenaar, J. C. A. Miller-Jones, R. N. Mohan, J. D. Mol, J. Morawietz, R. Morganti, D. D. Mulcahy, E. Mulder, H. Munk, L. Nieuwenhuis, R. van Nieuwpoort, J. E. Noordam, M. Norden, A. Noutsos, A. R. Offringa, H. Olofsson, A. Omar, E. Orrú, R. Overeem, H. Paas, M. Pandey-Pommier, V. N. Pandey, R. Pizzo, A. Polatidis, D. Rafferty, S. Rawlings, W. Reich, J. P. de Reijer, J. Reitsma, G. A. Renting, P. Riems, E. Rol, J. W. Romein, J. Roosjen, M. Ruiter, A. Scaife, K. van der Schaaf, B. Scheers, P. Schellart, A. Schoenmakers, G. Schoonderbeek, M. Serylak, A. Shulevski, J. Sluman, O. Smirnov, C. Sobey, H. Spreeuw, M. Steinmetz, C. G. M. Sterks, H. J. Stiepel, K. Stuurwold, M. Tagger, Y. Tang, C. Tasse, I. Thomas, S. Thoudam, M. C. Toribio, B. van der Tol, O. Usov, M. van Veelen, A. J. van der Veen, S. ter Veen, J. P. W. Verbiest, R. Vermeulen, N. Vermaas, C. Vocks, C. Vogt, M. de Vos, E. van der Wal, R. van Weeren, H. Weggemans, P. Weltvrede, S. White, S. J. Wijnholds, T. Wilhelmsson, O. Wucknitz, S. Yatawatta, P. Zarka, A. Zensus, and J. van Zwieten, “LOFAR: The LOw-Frequency ARray,” *A&A* **556**, A2 (2013), arXiv:1305.3550 [astro-ph.IM].
- [14] P. Zarka, J. N. Girard, M. Tagger, and L. Denis, “LSS/NenuFAR: The LOFAR Super Station project in Nançay,” in *SF2A-2012: Proceedings of the Annual meeting of the French Society of Astronomy and Astrophysics*, edited by S. Boissier, P. de Laverny, N. Nardetto, R. Samadi, D. Valls-Gabaud, and H. Wozniak (2012) pp. 687–694.
- [15] S. J. Tingay, R. Goeke, J. D. Bowman, D. Emrich, S. M. Ord, D. A. Mitchell, M. F. Morales, T. Booler, B. Crosse, R. B. Wayth, C. J. Lonsdale, S. Tremblay, D. Pallot, T. Colegate, A. Wicenec, N. Kudryavtseva, W. Arcus, D. Barnes, G. Bernardi, F. Briggs, S. Burns, J. D. Bunton, R. J. Cappallo, B. E. Corey, A. Deshpande, L. Desouza, B. M. Gaensler, L. J. Greenhill, P. J. Hall, B. J. Hazelton, D. Herne, J. N. Hewitt, M. Johnston-Hollitt, D. L. Kaplan, J. C. Kasper, B. B. Kincaid, R. Koenig, E. Kratzenberg, M. J. Lynch, B. McKinley, S. R. McWhirter, E. Morgan, D. Oberoi, J. Pathikulangara, T. Prabu, R. A. Remillard, A. E. E. Rogers, A. Roshi, J. E. Salah, R. J. Sault, N. Udaya-Shankar, F. Schlagenhauf, K. S. Srivani, J. Stevens, R. Subrahmanyam, M. Waterson, R. L. Webster, A. R. Whitney, A. Williams, C. L. Williams, and J. S. B. Wyithe, “The Murchison Widefield Array: The Square Kilometre Array Precursor at Low Radio Frequencies,” *PASA* **30**, e007 (2013), arXiv:1206.6945 [astro-ph.IM].
- [16] Randall B. Wayth, Steven J. Tingay, Cathryn M. Trott, David Emrich, Melanie Johnston-Hollitt, Ben McKinley, B. M. Gaensler, A. P. Beardsley, T. Booler, B. Crosse, T. M. O. Franzen, L. Horsley, D. L. Kaplan, D. Kenney, M. F. Morales, D. Pallot, G. Sleap, K. Steele, M. Walker, A. Williams, C. Wu, Iver. H. Cairns, M. D. Filipovic, S. Johnston, T. Murphy, P. Quinn, L. Staveley-Smith, R. Webster, and J. S. B. Wyithe, “The Phase II Murchison Widefield Array: Design overview,” *PASA* **35**, e033 (2018), arXiv:1809.06466 [astro-ph.IM].
- [17] Y. Gupta, B. Ajithkumar, H. S. Kale, S. Nayak, S. Sabhapathy, S. Sureshkumar, R. V. Swami, J. N. Chennalur, S. K. Ghosh, C. H. Ishwara-Chandra, B. C. Joshi, N. Kanekar, D. V. Lal, and S. Roy, “The upgraded GMRT: opening new windows on the radio Universe,” *Current Science* **113**, 707–714 (2017).
- [18] David R. DeBoer *et al.*, “Hydrogen Epoch of Reionization Array (HERA),” *Publ. Astron. Soc. Pac.* **129**, 045001 (2017), arXiv:1606.07473 [astro-ph.IM].
- [19] Lindsay M. Berkhou, Daniel C. Jacobs, Zuhra Abdurashidova, Tyrone Adams, James E. Aguirre, Paul Alexander, Zaki S. Ali, Rushelle Baartman, Yanga Balfour, Adam P. Beardsley, Gianni Bernardi, Tashalee S. Billings, Judd D. Bowman, Richard F. Bradley, Philip Bull, Jacob Burba, Steven Carey, Chris L. Carilli, Kai-Feng Chen, Carina Cheng, Samir Choudhuri, David R. DeBoer, Eloy de Lera Acedo, Matt Dexter, Joshua S. Dillon, Scott Dynes, Nico Eksteen, John Ely, Aaron Ewall-Wice, Nicolas Fagnoni, Randall Fritz, Steven R. Furlanetto, Kingsley Gale-Sides, Hugh Garsden, Bharat Kumar Gehlot, Abhik Ghosh, Brian Glendenning, Adelie Gorce, Deepthi Gorthi, Bradley Greig, Jasper Grobbelaar, Ziyaad Halday, Bryna J. Hazelton, Jacqueline N. Hewitt, Jack Hickish, Tian Huang, Alec Josaitis, Austin Julius, MacCalvin Kariseb, Nicholas S. Kern, Joshua Kerrigan, Honggeun Kim, Piyarat Kittiwisit, Saul A. Kohn, Matthew Kolopa-

- nis, Adam Lanman, Paul La Plante, Adrian Liu, Anita Loots, Yin-Zhe Ma, David Harold Edward MacMahon, Lourence Malan, Cresshim Malgas, Keith Malgas, Bradley Marero, Zachary E. Martinot, Andrei Mesinger, Mathakane Molewa, Miguel F. Morales, Tshegofalang Mosiane, Steven G. Murray, Abraham R. Neben, Bojan Nikolic, Chuneeta Devi Nunhokee, Hans Nuwegeld, Aaron R. Parsons, Robert Pascua, Nipanjana Patra, Samantha Pieterse, Yuxiang Qin, Eleanor Rath, Nima Razavi-Ghods, Daniel Riley, James Robnett, Kathryn Rosie, Mario G. Santos, Peter Sims, Saurabh Singh, Dara Storer, Hilton Swarts, Jianrong Tan, Nithyanandan Thyagarajan, Pieter van Wyngaarden, Peter K. G. Williams, Haoxuan Zheng, and Zhilei Xu, “Hydrogen Epoch of Reionization Array (HERA) Phase II Deployment and Commissioning,” arXiv e-prints, arXiv:2401.04304 (2024), arXiv:2401.04304 [astro-ph.IM].
- [20] Michael W. Eastwood, Marin M. Anderson, Ryan M. Monroe, Gregg Hallinan, Morgan Catha, Jayce Dowell, Hugh Garsden, Lincoln J. Greenhill, Brian C. Hicks, Jonathon Kocz, Danny C. Price, Frank K. Schinzel, Harish Vedantham, and Yuankun Wang, “The 21 cm Power Spectrum from the Cosmic Dawn: First Results from the OVRO-LWA,” AJ **158**, 84 (2019), arXiv:1906.08943 [astro-ph.CO].
- [21] L. Koopmans, J. Pritchard, G. Mellema, J. Aguirre, K. Ahn, R. Barkana, I. van Bemmel, G. Bernardi, A. Bonaldi, F. Briggs, A. G. de Bruyn, T. C. Chang, E. Chapman, X. Chen, B. Ciardi, P. Dayal, A. Ferrara, A. Fialkov, F. Fiore, K. Ichiki, I. T. Illiev, S. Inoue, V. Jelic, M. Jones, J. Lazio, U. Maio, S. Majumdar, K. J. Mack, A. Mesinger, M. F. Morales, A. Parsons, U. L. Pen, M. Santos, R. Schneider, B. Semelin, R. S. de Souza, R. Subrahmanyam, T. Takeuchi, H. Vedantham, J. Wagg, R. Webster, S. Wyithe, K. K. Datta, and C. Trott, “The Cosmic Dawn and Epoch of Reionisation with SKA,” in *Advancing Astrophysics with the Square Kilometre Array (AASKA14)* (2015) p. 1, arXiv:1505.07568 [astro-ph.CO].
- [22] Aaron R. Parsons, Adrian Liu, James E. Aguirre, Zaki S. Ali, Richard F. Bradley, Chris L. Carilli, David R. DeBoer, Matthew R. Dexter, Nicole E. Gugliucci, Daniel C. Jacobs, Pat Klima, David H. E. MacMahon, Jason R. Manley, David F. Moore, Jonathan C. Pober, Irina I. Stefan, and William P. Walbrugh, “New Limits on 21 cm Epoch of Reionization from PAPER-32 Consistent with an X-Ray Heated Intergalactic Medium at $z = 7.7$,” ApJ **788**, 106 (2014), arXiv:1304.4991 [astro-ph.CO].
- [23] Joshua S. Dillon, Adrian Liu, Christopher L. Williams, Jacqueline N. Hewitt, Max Tegmark, Edward H. Morgan, Alan M. Levine, Miguel F. Morales, Steven J. Tingay, Gianni Bernardi, Judd D. Bowman, Frank H. Briggs, Roger C. Cappallo, David Emrich, Daniel A. Mitchell, Divya Oberoi, Thiagaraj Prabu, Randall Wayth, and Rachel L. Webster, “Overcoming real-world obstacles in 21 cm power spectrum estimation: A method demonstration and results from early Murchison Widefield Array data,” Phys. Rev. D **89**, 023002 (2014), arXiv:1304.4229 [astro-ph.CO].
- [24] Joshua S. Dillon, Abraham R. Neben, Jacqueline N. Hewitt, Max Tegmark, N. Barry, A. P. Beardsley, J. D. Bowman, F. Briggs, P. Carroll, A. de Oliveira-Costa, A. Ewall-Wice, L. Feng, L. J. Greenhill, B. J. Hazelton, L. Hernquist, N. Hurley-Walker, D. C. Jacobs, H. S. Kim, P. Kittiwisit, E. Lenc, J. Line, A. Loeb, B. McKinley, D. A. Mitchell, M. F. Morales, A. R. Offringa, S. Paul, B. Pindor, J. C. Pober, P. Procopio, J. Riding, S. Sethi, N. Udaya Shankar, R. Subrahmanyam, I. Sullivan, Nithyanandan Thyagarajan, S. J. Tingay, C. Trott, R. B. Wayth, R. L. Webster, S. Wyithe, G. Bernardi, R. J. Cappallo, A. A. Deshpande, M. Johnston-Hollitt, D. L. Kaplan, C. J. Lonsdale, S. R. McWhirter, E. Morgan, D. Oberoi, S. M. Ord, T. Prabu, K. S. Srivani, A. Williams, and C. L. Williams, “Empirical covariance modeling for 21 cm power spectrum estimation: A method demonstration and new limits from early Murchison Widefield Array 128-tile data,” Phys. Rev. D **91**, 123011 (2015), arXiv:1506.01026 [astro-ph.CO].
- [25] A. Ewall-Wice, Joshua S. Dillon, J. N. Hewitt, A. Loeb, A. Mesinger, A. R. Neben, A. R. Offringa, M. Tegmark, N. Barry, A. P. Beardsley, G. Bernardi, Judd D. Bowman, F. Briggs, R. J. Cappallo, P. Carroll, B. E. Corey, A. de Oliveira-Costa, D. Emrich, L. Feng, B. M. Gaensler, R. Goeke, L. J. Greenhill, B. J. Hazelton, N. Hurley-Walker, M. Johnston-Hollitt, Daniel C. Jacobs, D. L. Kaplan, J. C. Kasper, HS Kim, E. Kratzenberg, E. Lenc, J. Line, C. J. Lonsdale, M. J. Lynch, B. McKinley, S. R. McWhirter, D. A. Mitchell, M. F. Morales, E. Morgan, Nithyanandan Thyagarajan, D. Oberoi, S. M. Ord, S. Paul, B. Pindor, J. C. Pober, T. Prabu, P. Procopio, J. Riding, A. E. E. Rogers, A. Roshi, N. Udaya Shankar, Shiv K. Sethi, K. S. Srivani, R. Subrahmanyam, I. S. Sullivan, S. J. Tingay, C. M. Trott, M. Waterson, R. B. Wayth, R. L. Webster, A. R. Whitney, A. Williams, C. L. Williams, C. Wu, and J. S. B. Wyithe, “First limits on the 21 cm power spectrum during the Epoch of X-ray heating,” MNRAS **460**, 4320–4347 (2016), arXiv:1605.00016 [astro-ph.CO].
- [26] A. P. Beardsley, B. J. Hazelton, I. S. Sullivan, P. Carroll, N. Barry, M. Rahimi, B. Pindor, C. M. Trott, J. Line, Daniel C. Jacobs, M. F. Morales, J. C. Pober, G. Bernardi, Judd D. Bowman, M. P. Busch, F. Briggs, R. J. Cappallo, B. E. Corey, A. de Oliveira-Costa, Joshua S. Dillon, D. Emrich, A. Ewall-Wice, L. Feng, B. M. Gaensler, R. Goeke, L. J. Greenhill, J. N. Hewitt, N. Hurley-Walker, M. Johnston-Hollitt, D. L. Kaplan, J. C. Kasper, H. S. Kim, E. Kratzenberg, E. Lenc, A. Loeb, C. J. Lonsdale, M. J. Lynch, B. McKinley, S. R. McWhirter, D. A. Mitchell, E. Morgan, A. R. Neben, Nithyanandan Thyagarajan, D. Oberoi, A. R. Offringa, S. M. Ord, S. Paul, T. Prabu, P. Procopio, J. Riding, A. E. E. Rogers, A. Roshi, N. Udaya Shankar, Shiv K. Sethi, K. S. Srivani, R. Subrahmanyam, M. Tegmark, S. J. Tingay, M. Waterson, R. B. Wayth, R. L. Webster, A. R. Whitney, A. Williams, C. L. Williams, C. Wu, and J. S. B. Wyithe, “First Season MWA EoR Power spectrum Results at Redshift 7,” ApJ **833**, 102 (2016), arXiv:1608.06281 [astro-ph.IM].
- [27] A.~H. Patil, S. Yatawatta, L.~V.~E. Koopmans, A.~G. de Bruyn, M.~A. Brentjens, S. Zaroubi, K.~M.~B. Asad, M. Hatef, V. Jelić, M. Mevius, A.~R. Offringa, V.~N. Pandey, H. Vedantham, F.~B. Abdalla, W.~N. Brouw, E Chapman, B Ciardi, B.~K. Gehlot, A Ghosh, G Harker, I.~T. Iliev, K Kakiichi, S Majumdar, G Mellema, M.~B. Silva, J Schaye, D Vrbanec, and

- S.~J. Wijnholds, “Upper Limits on the 21 cm Epoch of Reionization Power Spectrum from One Night with LOFAR,” *ApJ* **838**, 65 (2017), arXiv:1702.08679.
- [28] W. Li, J. C. Pober, N. Barry, B. J. Hazelton, M. F. Morales, C. M. Trott, A. Lanman, M. Wilensky, I. Sullivan, A. P. Beardsley, T. Booler, J. D. Bowman, R. Byrne, B. Crosse, D. Emrich, T. M. O. Franzen, K. Hasegawa, L. Horsley, M. Johnston-Hollitt, D. C. Jacobs, C. H. Jordan, R. C. Joseph, T. Kaneiji, D. L. Kaplan, D. Kenney, K. Kubota, J. Line, C. Lynch, B. McKinley, D. A. Mitchell, S. Murray, D. Pallot, B. Pindor, M. Rahimi, J. Riding, G. Sleap, K. Steele, K. Takahashi, S. J. Tingay, M. Walker, R. B. Wayth, R. L. Webster, A. Williams, C. Wu, J. S. B. Wyithe, S. Yoshiura, and Q. Zheng, “First Season MWA Phase II Epoch of Reionization Power Spectrum Results at Redshift 7,” *ApJ* **887**, 141 (2019), arXiv:1911.10216 [astro-ph.CO].
- [29] N. Barry, M. Wilensky, C. M. Trott, B. Pindor, A. P. Beardsley, B. J. Hazelton, I. S. Sullivan, M. F. Morales, J. C. Pober, J. Line, B. Greig, R. Byrne, A. Lanman, W. Li, C. H. Jordan, R. C. Joseph, B. McKinley, M. Rahimi, S. Yoshiura, J. D. Bowman, B. M. Gaensler, J. N. Hewitt, D. C. Jacobs, D. A. Mitchell, N. Udaya Shankar, S. K. Sethi, R. Subrahmanyam, S. J. Tingay, R. L. Webster, and J. S. B. Wyithe, “Improving the Epoch of Reionization Power Spectrum Results from Murchison Widefield Array Season 1 Observations,” *ApJ* **884**, 1 (2019), arXiv:1909.00561 [astro-ph.IM].
- [30] B. K. Gehlot, F. G. Mertens, L. V. E. Koopmans, M. A. Brentjens, S. Zaroubi, B. Ciardi, A. Ghosh, M. Hatef, I. T. Iliev, Jelić, V., R. Kooistra, F. Krause, G. Mellema, M. Mevius, M. Mitra, A. R. Offringa, V. N. Pandey, A. M. Sardarabadi, J. Schaye, M. B. Silva, H. K. Vedantham, and S. Yatawatta, “The first power spectrum limit on the 21-cm signal of neutral hydrogen during the Cosmic Dawn at $z = 20\text{--}25$ from LOFAR,” *MNRAS* **488**, 4271–4287 (2019), arXiv:1809.06661 [astro-ph.IM].
- [31] Matthew Kolopanis, Daniel C. Jacobs, Carina Cheng, Aaron R. Parsons, Saul A. Kohn, Jonathan C. Pober, James E. Aguirre, Zaki S. Ali, Gianni Bernardi, Richard F. Bradley, Chris L. Carilli, David R. DeBoer, Matthew R. Dexter, Joshua S. Dillon, Joshua Kerrigan, Pat Klima, Adrian Liu, David H. E. MacMahon, David F. Moore, Nithyanandan Thyagarajan, Chuneeta D. Nunhokee, William P. Walbrugh, and Andre Walker, “A Simplified, Lossless Reanalysis of PAPER-64,” *ApJ* **883**, 133 (2019), arXiv:1909.02085 [astro-ph.CO].
- [32] Cathryn M. Trott, C. H. Jordan, S. Midgley, N. Barry, B. Greig, B. Pindor, J. H. Cook, G. Sleap, S. J. Tingay, D. Ung, P. Hancock, A. Williams, J. Bowman, R. Byrne, A. Chokshi, B. J. Hazelton, K. Hasegawa, D. Jacobs, R. C. Joseph, W. Li, JLB Line, C. Lynch, B. McKinley, D. A. Mitchell, M. F. Morales, M. Ouchi, J. C. Pober, M. Rahimi, K. Takahashi, R. B. Wayth, R. L. Webster, M. Wilensky, J. S. B. Wyithe, S. Yoshiura, Z. Zhang, and Q. Zheng, “Deep multi-redshift limits on Epoch of Reionisation 21 cm Power Spectra from Four Seasons of Murchison Widefield Array Observations,” *MNRAS* (2020), 10.1093/mnras/staa414, arXiv:2002.02575 [astro-ph.CO].
- [33] F. G. Mertens *et al.*, “Improved upper limits on the 21-cm signal power spectrum of neutral hydrogen at $z \approx 9.1$ from LOFAR,” *Mon. Not. Roy. Astron. Soc.* **493**, 1662–1685 (2020), arXiv:2002.07196 [astro-ph.CO].
- [34] H. Garsden, L. Greenhill, G. Bernardi, A. Fialkov, D. C. Price, D. Mitchell, J. Dowell, M. Spinelli, and F. K. Schinzel, “A 21-cm power spectrum at 48 MHz, using the Owens Valley Long Wavelength Array,” *MNRAS* **506**, 5802–5817 (2021), arXiv:2102.09596 [astro-ph.CO].
- [35] S. Yoshiura, B. Pindor, J. L. B. Line, N. Barry, C. M. Trott, A. Beardsley, J. Bowman, R. Byrne, A. Chokshi, B. J. Hazelton, K. Hasegawa, E. Howard, B. Greig, D. Jacobs, C. H. Jordan, R. Joseph, M. Kolopanis, C. Lynch, B. McKinley, D. A. Mitchell, M. F. Morales, S. G. Murray, J. C. Pober, M. Rahimi, K. Takahashi, S. J. Tingay, R. B. Wayth, R. L. Webster, M. Wilensky, J. S. B. Wyithe, Z. Zhang, and Q. Zheng, “A new MWA limit on the 21 cm power spectrum at redshifts 13–17,” *MNRAS* **505**, 4775–4790 (2021), arXiv:2105.12888 [astro-ph.CO].
- [36] Zara Abdurashidova, James E. Aguirre, Paul Alexander, Zaki S. Ali, Yanga Balfour, Adam P. Beardsley, Gianni Bernardi, Tashalee S. Billings, Judd D. Bowman, Richard F. Bradley, Philip Bull, Jacob Burba, Steve Carey, Chris L. Carilli, Carina Cheng, David R. DeBoer, Matt Dexter, Eloy de Lera Acedo, Taylor Dibblee-Barkman, Joshua S. Dillon, John Ely, Aaron Ewall-Wice, Nicolas Fagnoni, Randall Fritz, Steven R. Furlanetto, Kingsley Gale-Sides, Brian Glendenning, Deepthi Gorthi, Bradley Greig, Jasper Grobbelaar, Ziyaad Halday, Bryna J. Hazelton, Jacqueline N. Hewitt, Jack Hickish, Daniel C. Jacobs, Austin Julius, Nicholas S. Kern, Joshua Kerrigan, Piyanat Kittiwit, Saul A. Kohn, Matthew Kolopanis, Adam Lanman, Paul La Plante, Telalo Lekalake, David Lewis, Adrian Liu, David MacMahon, Lourence Malan, Cresshim Malgas, Matthys Maree, Zachary E. Martinot, Eunice Matsetela, Andrei Mesinger, Mathakane Molewa, Miguel F. Morales, Tshegofalang Mosiane, Steven G. Murray, Abraham R. Neben, Bojan Nikolic, Chuneeta D. Nunhokee, Aaron R. Parsons, Nipanjana Patra, Robert Pascua, Samantha Pieterse, Jonathan C. Pober, Nima Razavi-Ghods, Jon Ringuelette, James Robnett, Kathryn Rosie, Peter Sims, Saurabh Singh, Craig Smith, Angelo Syce, Nithyanandan Thyagarajan, Peter K. G. Williams, Haoxuan Zheng, and HERA Collaboration, “First Results from HERA Phase I: Upper Limits on the Epoch of Reionization 21 cm Power Spectrum,” *ApJ* **925**, 221 (2022), arXiv:2108.02263 [astro-ph.CO].
- [37] HERA Collaboration, Zara Abdurashidova, Tyrone Adams, James E. Aguirre, Paul Alexander, Zaki S. Ali, Rushelle Baartman, Yanga Balfour, Rennan Barkana, Adam P. Beardsley, Gianni Bernardi, Tashalee S. Billings, Judd D. Bowman, Richard F. Bradley, Daniela Breitman, Philip Bull, Jacob Burba, Steve Carey, Chris L. Carilli, Carina Cheng, Samir Choudhuri, David R. DeBoer, Eloy de Lera Acedo, Matt Dexter, Joshua S. Dillon, John Ely, Aaron Ewall-Wice, Nicolas Fagnoni, Anastasia Fialkov, Randall Fritz, Steven R. Furlanetto, Kingsley Gale-Sides, Hugh Garsden, Brian Glendenning, Adélie Gorce, Deepthi Gorthi, Bradley Greig, Jasper Grobbelaar, Ziyaad Hal-

- day, Bryna J. Hazelton, Stefan Heimersheim, Jacqueline N. Hewitt, Jack Hickish, Daniel C. Jacobs, Austin Julius, Nicholas S. Kern, Joshua Kerrigan, Piyanat Kittiwisit, Saul A. Kohn, Matthew Kolopanis, Adam Lanman, Paul La Plante, David Lewis, Adrian Liu, Anita Loots, Yin-Zhe Ma, David H. E. MacMahon, Lourence Malan, Keith Malgas, Cresshim Malgas, Matthys Maree, Bradley Marero, Zachary E. Martinot, Lisa McBride, Andrei Mesinger, Jordan Mirocha, Mathakane Molewa, Miguel F. Morales, Tshegofalang Mosiane, Julian B. Muñoz, Steven G. Murray, Vighnesh Nagpal, Abraham R. Neben, Bojan Nikolic, Chuneeta D. Nunhokee, Hans Nuwegeld, Aaron R. Parsons, Robert Pascua, Nipanjana Patra, Samantha Pieterse, Yuxiang Qin, Nima Razavi-Ghods, James Robnett, Kathryn Rosie, Mario G. Santos, Peter Sims, Saurabh Singh, Craig Smith, Hilton Swarts, Jianrong Tan, Nithyanandan Thyagarajan, Michael J. Wilensky, Peter K. G. Williams, Pieter van Wyngaarden, and Haoxuan Zheng, “Improved Constraints on the 21 cm EoR Power Spectrum and the X-Ray Heating of the IGM with HERA Phase I Observations,” *ApJ* **945**, 124 (2023).
- [38] Michael J. Wilensky, Miguel F. Morales, Bryna J. Hazelton, Pyxie L. Star, Nichole Barry, Ruby Byrne, C. H. Jordan, Daniel C. Jacobs, Jonathan C. Pober, and C. M. Trott, “Evidence of Ultrafaint Radio Frequency Interference in Deep 21 cm Epoch of Reionization Power Spectra with the Murchison Wide-field Array,” *ApJ* **957**, 78 (2023), arXiv:2310.03851 [astro-ph.CO].
- [39] S. Munshi, F. G. Mertens, L. V. E. Koopmans, A. R. Offringa, B. Semelin, D. Aubert, R. Barkana, A. Bracco, S. A. Brackenhoff, B. Cecconi, E. Ceccotti, S. Corbel, A. Fialkov, B. K. Gehlot, R. Ghara, J. N. Girard, J. M. Grießmeier, C. Höfer, I. Hothi, R. Mériot, M. Mevius, P. Ocvirk, A. K. Shaw, G. Theureau, S. Yatawatta, P. Zarka, and S. Zaroubi, “First upper limits on the 21 cm signal power spectrum from cosmic dawn from one night of observations with NenuFAR,” *A&A* **681**, A62 (2024), arXiv:2311.05364 [astro-ph.CO].
- [40] Anshuman Acharya, Florent Mertens, Benedetta Ciardì, Raghunath Ghara, Léon V. E. Koopmans, and Saleem Zaroubi, “Revised LOFAR upper limits on the 21-cm signal power spectrum at $z \approx 9.1$ using machine learning and gaussian process regression,” *MNRAS* **534**, L30–L34 (2024), arXiv:2408.10051 [astro-ph.CO].
- [41] F. G. Mertens *et al.*, “Deeper multi-redshift upper limits on the Epoch of Reionization 21-cm signal power spectrum from LOFAR between $z=8.3$ and $z=10.1$,” *Astron. Astrophys.* **698**, A186 (2025), arXiv:2503.05576 [astro-ph.CO].
- [42] C. D. Nunhokee *et al.*, “Limits on the 21 cm Power Spectrum at $z = 6.5\text{--}7.0$ from Murchison Widefield Array Observations,” *Astrophys. J.* **989**, 57 (2025), arXiv:2505.09097 [astro-ph.CO].
- [43] Zara Abdurashidova, James E. Aguirre, Paul Alexander, Zaki S. Ali, Yanga Balfour, Rennan Barkana, Adam P. Beardsley, Gianni Bernardi, Tashalee S. Billings, Judd D. Bowman, Richard F. Bradley, Philip Bull, Jacob Burba, Steve Carey, Chris L. Carilli, Carina Cheng, David R. DeBoer, Matt Dexter, Eloy de Lera Acedo, Joshua S. Dillon, John Ely, Aaron Ewall-Wice, Nicolas Fagnoni, Anastasia Fialkov, Randall Fritz, Steven R. Furlanetto, Kingsley Gale-Sides, Brian Glendenning, Deepthi Gorthi, Bradley Greig, Jasper Grobbelaar, Ziyaad Halday, Bryna J. Hazelton, Stefan Heimersheim, Jacqueline N. Hewitt, Jack Hickish, Daniel C. Jacobs, Austin Julius, Nicholas S. Kern, Joshua Kerrigan, Piyanat Kittiwisit, Saul A. Kohn, Matthew Kolopanis, Adam Lanman, Paul La Plante, Telalo Lekalake, David Lewis, Adrian Liu, Yin-Zhe Ma, David MacMahon, Lourence Malan, Cresshim Malgas, Matthys Maree, Zachary E. Martinot, Eu-nice Matsetela, Andrei Mesinger, Jordan Mirocha, Mathakane Molewa, Miguel F. Morales, Tshegofalang Mosiane, Julian B. Muñoz, Steven G. Murray, Abraham R. Neben, Bojan Nikolic, Chuneeta D. Nunhokee, Aaron R. Parsons, Nipanjana Patra, Samantha Pieterse, Jonathan C. Pober, Yuxiang Qin, Nima Razavi-Ghods, Itamar Reis, Jon Ringuette, James Robnett, Kathryn Rosie, Mario G. Santos, Sudipta Sikder, Peter Sims, Craig Smith, Angelo Syce, Nithyanandan Thyagarajan, Peter K. G. Williams, and Haoxuan Zheng, “HERA Phase I Limits on the Cosmic 21 cm Signal: Constraints on Astrophysics and Cosmology during the Epoch of Reionization,” *ApJ* **924**, 51 (2022), arXiv:2108.07282 [astro-ph.CO].
- [44] R. Ghara *et al.*, “Constraints on the state of the intergalactic medium at $z \sim 8 - 10$ using redshifted 21 cm observations with LOFAR,” *Astron. Astrophys.* **699**, A109 (2025), arXiv:2505.00373 [astro-ph.CO].
- [45] Adrian Liu and J. Richard Shaw, “Data Analysis for Precision 21 cm Cosmology,” *PASP* **132**, 062001 (2020), arXiv:1907.08211 [astro-ph.IM].
- [46] A. Datta, J. D. Bowman, and C. L. Carilli, “Bright Source Subtraction Requirements for Redshifted 21 cm Measurements,” *ApJ* **724**, 526–538 (2010), arXiv:1005.4071 [astro-ph.CO].
- [47] Miguel F. Morales, Bryna Hazelton, Ian Sullivan, and Adam Beardsley, “Four Fundamental Foreground Power Spectrum Shapes for 21 cm Cosmology Observations,” *ApJ* **752**, 137 (2012), arXiv:1202.3830 [astro-ph.IM].
- [48] Aaron R. Parsons, Jonathan C. Pober, James E. Aguirre, Christopher L. Carilli, Daniel C. Jacobs, and David F. Moore, “A Per-baseline, Delay-spectrum Technique for Accessing the 21 cm Cosmic Reionization Signature,” *ApJ* **756**, 165 (2012), arXiv:1204.4749 [astro-ph.IM].
- [49] Nithyanandan Thyagarajan *et al.*, “Confirmation of Wide-Field Signatures in Redshifted 21 cm Power Spectra,” *Astrophys. J. Lett.* **807**, L28 (2015), arXiv:1506.06150 [astro-ph.CO].
- [50] Adrian Liu, Aaron R. Parsons, and Cathryn M. Trott, “Epoch of reionization window. I. Mathematical formalism,” *Phys. Rev. D* **90**, 023018 (2014), arXiv:1404.2596 [astro-ph.CO].
- [51] Adrian Liu, Aaron R. Parsons, and Cathryn M. Trott, “Epoch of reionization window. II. Statistical methods for foreground wedge reduction,” *Phys. Rev. D* **90**, 023019 (2014), arXiv:1404.4372 [astro-ph.CO].
- [52] S. Munshi, F. G. Mertens, L. V. E. Koopmans, A. R. Offringa, E. Ceccotti, S. A. Brackenhoff, J. K. Chege, B. K. Gehlot, S. Ghosh, C. Höfer, and M. Mevius, “Beyond the horizon: Quantifying the full sky foreground wedge in the cylindrical power spectrum,” *A&A* **693**, A276 (2025), arXiv:2407.10686 [astro-ph.CO].
- [53] Adrian Liu and Max Tegmark, “A method for 21 cm power spectrum estimation in the presence of foregrounds,” *Phys. Rev. D* **83**, 103006 (2011),

- arXiv:1103.0281 [astro-ph.CO].
- [54] Emma Chapman, Filipe B. Abdalla, Geraint Harker, Vibor Jelić, Panagiotis Labropoulos, Saleem Zaroubi, Michiel A. Brentjens, A. G. de Bruyn, and L. V. E. Koopmans, “Foreground removal using FASTICA: a showcase of LOFAR-EoR,” *MNRAS* **423**, 2518–2532 (2012), arXiv:1201.2190 [astro-ph.CO].
- [55] Abhik Ghosh, Léon V. E. Koopmans, E. Chapman, and V. Jelić, “A Bayesian analysis of redshifted 21-cm H I signal and foregrounds: simulations for LOFAR,” *MNRAS* **452**, 1587–1600 (2015), arXiv:1506.04982 [astro-ph.CO].
- [56] Aaron Ewall-Wice, Nicholas Kern, Joshua S. Dillon, Adrian Liu, Aaron Parsons, Saurabh Singh, Adam Lanman, Paul La Plante, Nicolas Fagnoni, Eloy de Lera Acedo, David R. DeBoer, Chuneeta Nunhokee, Philip Bull, Tzu-Ching Chang, T. Joseph W. Lazio, James Aguirre, and Sean Weinberg, “DAYENU: a simple filter of smooth foregrounds for intensity mapping power spectra,” *MNRAS* **500**, 5195–5213 (2021), arXiv:2004.11397 [astro-ph.CO].
- [57] F. G. Mertens, A. Ghosh, and L. V. E. Koopmans, “Statistical 21-cm signal separation via Gaussian Process Regression analysis,” *MNRAS* **478**, 3640–3652 (2018), arXiv:1711.10834 [astro-ph.CO].
- [58] Haochen Wang, Kiyoshi Masui, Kevin Bandura, Arnab Chakraborty, Matt Dobbs, Simon Foreman, Liam Gray, Mark Halpern, Albin Joseph, Joshua MacEachern, Juan Mena-Parra, Kyle Miller, Laura Newburgh, Sourabh Paul, Alex Reda, Pranav Sanghavi, Seth Siegel, and Dallas Wulf, “Demonstration of hybrid foreground removal on CHIME data,” arXiv e-prints , arXiv:2408.08949 (2024), arXiv:2408.08949 [astro-ph.CO].
- [59] N. Barry, B. Hazelton, I. Sullivan, M. F. Morales, and J. C. Pober, “Calibration requirements for detecting the 21 cm epoch of reionization power spectrum and implications for the SKA,” *MNRAS* **461**, 3135–3144 (2016), arXiv:1603.00607 [astro-ph.IM].
- [60] Ajinkya H. Patil, Sarod Yatawatta, Saleem Zaroubi, Léon V. E. Koopmans, A. G. de Bruyn, Vibor Jelić, Benedetta Ciardi, Ilian T. Iliev, Maaijke Mevius, Vishambhar N. Pandey, and Bharat K. Gehlot, “Systematic biases in low-frequency radio interferometric data due to calibration: the LOFAR-EoR case,” *MNRAS* **463**, 4317–4330 (2016), arXiv:1605.07619 [astro-ph.IM].
- [61] Aaron Ewall-Wice, Joshua S. Dillon, Adrian Liu, and Jacqueline Hewitt, “The impact of modelling errors on interferometer calibration for 21 cm power spectra,” *MNRAS* **470**, 1849–1870 (2017), arXiv:1610.02689 [astro-ph.CO].
- [62] Ruby Byrne, Miguel F. Morales, Bryna Hazelton, Wenyang Li, Nichole Barry, Adam P. Beardsley, Ronny Joseph, Jonathan Pober, Ian Sullivan, and Kathryn Trott, “Fundamental Limitations on the Calibration of Redundant 21 cm Cosmology Instruments and Implications for HERA and the SKA,” *ApJ* **875**, 70 (2019), arXiv:1811.01378 [astro-ph.IM].
- [63] A. Mouri Sardarabadi and L. V. E. Koopmans, “Quantifying suppression of the cosmological 21-cm signal due to direction-dependent gain calibration in radio interferometers,” *MNRAS* **483**, 5480–5490 (2019), arXiv:1809.03755 [astro-ph.IM].
- [64] Abraham R. Neben, Jacqueline N. Hewitt, Richard F. Bradley, Joshua S. Dillon, G. Bernardi, J. D. Bowman, F. Briggs, R. J. Cappallo, B. E. Corey, A. A. Deshpande, R. Goeke, L. J. Greenhill, B. J. Hazelton, M. Johnston-Hollitt, D. L. Kaplan, C. J. Lonsdale, S. R. McWhirter, D. A. Mitchell, M. F. Morales, E. Morgan, D. Oberoi, S. M. Ord, T. Prabu, N. Udaya Shankar, K. S. Srivani, R. Subrahmanyan, S. J. Tingay, R. B. Wayth, R. L. Webster, A. Williams, and C. L. Williams, “Beam-forming Errors in Murchison Wide-field Array Phased Array Antennas and their Effects on Epoch of Reionization Science,” *ApJ* **820**, 44 (2016), arXiv:1602.05249 [astro-ph.IM].
- [65] Ronniy C. Joseph, Kathryn M. Trott, and Randall B. Wayth, “The Bias and Uncertainty of Redundant and Sky-based Calibration Under Realistic Sky and Telescope Conditions,” *AJ* **156**, 285 (2018), arXiv:1810.11237 [astro-ph.IM].
- [66] T. Ansah-Narh, F. B. Abdalla, O. M. Smirnov, K. M. B. Asad, and J. R. Shaw, “Simulations of systematic direction-dependent instrumental effects in intensity mapping experiments,” *MNRAS* **481**, 2694–2710 (2018).
- [67] H. Zheng *et al.*, “Brute-force mapmaking with compact interferometers: a MITEoR northern sky map from 128 to 175 MHz,” *Mon. Not. Roy. Astron. Soc.* **465**, 2901–2915 (2017), arXiv:1605.03980 [astro-ph.IM].
- [68] Naomi Orosz, Joshua S. Dillon, Aaron Ewall-Wice, Aaron R. Parsons, and Nithyanandan Thyagarajan, “Mitigating the effects of antenna-to-antenna variation on redundant-baseline calibration for 21 cm cosmology,” *MNRAS* **487**, 537–549 (2019), arXiv:1809.09728 [astro-ph.CO].
- [69] Ronniy C. Joseph, C. M. Trott, R. B. Wayth, and A. Nasirudin, “Calibration and 21-cm power spectrum estimation in the presence of antenna beam variations,” *MNRAS* **492**, 2017–2028 (2020), arXiv:1911.13088 [astro-ph.IM].
- [70] Samir Choudhuri, Philip Bull, and Hugh Garsden, “Patterns of primary beam non-redundancy in close-packed 21 cm array observations,” *MNRAS* **506**, 2066–2088 (2021), arXiv:2101.02684 [astro-ph.CO].
- [71] Honggeun Kim, Bang D. Nhan, Jacqueline N. Hewitt, Nicholas S. Kern, Joshua S. Dillon, Eloy de Lera Acedo, Scott B. C. Dynes, Nivedita Mahesh, Nicolas Fagnoni, and David R. DeBoer, “The Impact of Beam Variations on Power Spectrum Estimation for 21 cm Cosmology. I. Simulations of Foreground Contamination for HERA,” *ApJ* **941**, 207 (2022), arXiv:2210.16421 [astro-ph.IM].
- [72] Nicholas S. Kern, Aaron R. Parsons, Joshua S. Dillon, Adam E. Lanman, Nicolas Fagnoni, and Eloy de Lera Acedo, “Mitigating Internal Instrument Coupling for 21 cm Cosmology I: Temporal and Spectral Modeling in Simulations,” arXiv e-prints , arXiv:1909.11732 (2019), arXiv:1909.11732 [astro-ph.IM].
- [73] Daniel C. X. Ung, Marcin Sokolowski, Adrian T. Sutinjo, and David B. Davidson, “Noise Temperature of Phased Array Radio Telescope: The Murchison Wide-field Array and the Engineering Development Array,” *IEEE Transactions on Antennas and Propagation* **68**, 5395–5404 (2020), arXiv:2003.05116 [astro-ph.IM].
- [74] Alec T. Josaitis, Aaron Ewall-Wice, Nicolas Fagnoni, and Eloy de Lera Acedo, “Array element coupling in radio interferometry I: a semi-analytic approach,” *MNRAS*

- RAS **514**, 1804–1827 (2022), arXiv:2110.10879 [astro-ph.IM].
- [75] E. Rath, R. Pascua, A. T. Josaitis, A. Ewall-Wice, N. Fagnoni, E. de Lera Acedo, Z. E. Martinot, Z. Abdurashidova, T. Adams, J. E. Aguirre, R. Baartman, A. P. Beardsley, L. M. Berkhout, G. Bernardi, T. S. Billings, J. D. Bowman, P. Bull, J. Burba, R. Byrne, S. Carey, K. F. Chen, S. Choudhuri, T. Cox, D. R. DeBoer, M. Dexter, J. S. Dillon, S. Dynes, N. Eksteen, J. Ely, R. Fritz, S. R. Furlanetto, K. Gale-Sides, H. Garsden, B. K. Gehlot, A. Ghosh, A. Gorce, D. Gorthi, Z. Halday, B. J. Hazelton, J. N. Hewitt, J. Hickish, T. Huang, D. C. Jacobs, N. S. Kern, J. Kerriigan, P. Kittiwisit, M. Kolopanis, A. Lanman, A. Liu, Y. Z. Ma, D. H. E. MacMahon, L. Malan, C. Malgas, K. Malgas, B. Marero, L. McBride, A. Mesinger, N. Mohamed-Hinds, M. Molewa, M. F. Morales, S. G. Murray, B. Nikolic, H. Nuwegeld, A. R. Parsons, N. Patra, P. La Plante, Y. Qin, N. Razavi-Ghods, D. Riley, J. Robnett, K. Rosie, M. G. Santos, P. Sims, S. Singh, D. Storer, H. Swarts, J. Tan, M. J. Wilensky, P. K. G. Williams, P. van Wyngaarden, and H. Zheng, “Investigating Mutual Coupling in the Hydrogen Epoch of Reionization Array and Mitigating its Effects on the 21-cm Power Spectrum,” arXiv e-prints , arXiv:2406.08549 (2024), arXiv:2406.08549 [astro-ph.CO].
- [76] Kai-Feng Chen, Michael J. Wilensky, Adrian Liu, Joshua S. Dillon, Jacqueline N. Hewitt, Tyrone Adams, James E. Aguirre, Rushelle Baartman, Adam P. Beardsley, Lindsay M. Berkhout, Gianni Bernardi, Tashalee S. Billings, Judd D. Bowman, Philip Bull, Jacob Burba, Ruby Byrne, Steven Carey, Samir Choudhuri, Tyler Cox, David. R. DeBoer, Matt Dexter, Nico Eksteen, John Ely, Aaron Ewall-Wice, Steven R. Furlanetto, Kingsley Gale-Sides, Hugh Garsden, Bharat Kumar Gehlot, Adélie Gorce, Deepthi Gorthi, Ziyaad Halday, Bryna J. Hazelton, Jack Hickish, Daniel C. Jacobs, Alec Josaitis, Nicholas S. Kern, Joshua Kerrigan, Piyanat Kittiwisit, Matthew Kolopanis, Paul La Plante, Adam Lanman, Yin-Zhe Ma, David H. E. MacMahon, Lourence Malan, Cresshim Malgas, Keith Malgas, Bradley Marero, Zachary E. Martinot, Lisa McBride, Andrei Mesinger, Nicel Mohamed-Hinds, Mathakane Molewa, Miguel F. Morales, Steven G. Murray, Hans Nuwegeld, Aaron R. Parsons, Robert Pascua, Yuxiang Qin, Eleanor Rath, Nima Razavi-Ghods, James Robnett, Mario G. Santos, Peter Sims, Saurabh Singh, Dara Storer, Hilton Swarts, Jianrong Tan, Pieter van Wyngaarden, and Haoxuan Zheng, “Impacts and Statistical Mitigation of Missing Data on the 21 cm Power Spectrum: A Case Study with the Hydrogen Epoch of Reionization Array,” ApJ **979**, 191 (2025), arXiv:2411.10529 [astro-ph.CO].
- [77] Harish Vedantham, N. Udaya Shankar, and Ravi Subrahmanyam, “Imaging the Epoch of Reionization: Limitations from Foreground Confusion and Imaging Algorithms,” ApJ **745**, 176 (2012), arXiv:1106.1297 [astro-ph.IM].
- [78] Cathryn M. Trott, Randall B. Wayth, and Steven J. Tingay, “The impact of point source subtraction residuals on 21 cm Epoch of Reionization estimation,” Astrophys. J. **757**, 101 (2012), arXiv:1208.0646 [astro-ph.CO].
- [79] Bryna J. Hazelton, Miguel F. Morales, and Ian S. Sullivan, “The Fundamental Multi-baseline Mode-mixing Foreground in 21 cm Epoch of Reionization Observations,” ApJ **770**, 156 (2013), arXiv:1301.3126 [astro-ph.IM].
- [80] Nithyanandan Thyagarajan *et al.*, “A Study of Fundamental Limitations to Statistical Detection of Redshifted H I from the Epoch of Reionization,” Astrophys. J. **776**, 6 (2013), arXiv:1308.0565 [astro-ph.CO].
- [81] Adrian Liu, Aaron R. Parsons, and Cathryn M. Trott, “Epoch of reionization window. I. Mathematical formalism,” Phys. Rev. D **90**, 023018 (2014), arXiv:1404.2596 [astro-ph.CO].
- [82] Paul La Plante, Jordan Mirocha, Adélie Gorce, Adam Lidz, and Aaron Parsons, “Prospects for 21 cm Galaxy Cross-correlations with HERA and the Roman High-latitude Survey,” Astrophys. J. **944**, 59 (2023), arXiv:2205.09770 [astro-ph.CO].
- [83] Samuel Gagnon-Hartman, James Davies, and Andrei Mesinger, “Detecting galaxy-21-cm cross-correlation during reionization,” arXiv e-prints , arXiv:2502.20447 (2025), arXiv:2502.20447 [astro-ph.CO].
- [84] Hannah Fronenberg and Adrian Liu, “Forecasts and Statistical Insights for Line Intensity Mapping Cross-correlations: A Case Study with 21 cm × [C II],” ApJ **975**, 222 (2024), arXiv:2407.14588 [astro-ph.CO].
- [85] Hong-Ming Zhu, Ue-Li Pen, Yu Yu, Xinzong Er, and Xuelei Chen, “Cosmic tidal reconstruction,” Phys. Rev. D **93**, 103504 (2016), arXiv:1511.04680 [astro-ph.CO].
- [86] Hong-Ming Zhu, Tian-Xiang Mao, and Ue-Li Pen, “Cosmic Tidal Reconstruction with Halo Fields,” Astrophys. J. **929**, 5 (2022), arXiv:2108.01575 [astro-ph.CO].
- [87] Shi-Hui Zang, Hong-Ming Zhu, Marcel Schmittfull, and Ue-Li Pen, “Cosmic Tidal Reconstruction in Redshift Space,” Astrophys. J. **962**, 21 (2024), arXiv:2212.04294 [astro-ph.CO].
- [88] Hong-Ming Zhu, Ue-Li Pen, Yu Yu, and Xuelei Chen, “Recovering lost 21 cm radial modes via cosmic tidal reconstruction,” Phys. Rev. D **98**, 043511 (2018), arXiv:1610.07062 [astro-ph.CO].
- [89] Naim Göksel Karaçaylı and Nikhil Padmanabhan, “Anatomy of cosmic tidal reconstruction,” MNRAS **486**, 3864–3873 (2019), arXiv:1904.01387 [astro-ph.CO].
- [90] Omar Darwish, Simon Foreman, Muntazir M. Abidi, Tobias Baldauf, Blake D. Sherwin, and P. Daniel Meerbburg, “Density reconstruction from biased tracers and its application to primordial non-Gaussianity,” Phys. Rev. D **104**, 123520 (2021), arXiv:2007.08472 [astro-ph.CO].
- [91] Samuel Gagnon-Hartman, Yue Cui, Adrian Liu, Siyamak Ravanbakhsh, and Jacob Kennedy, “Recovering the wedge modes lost to 21-cm foregrounds,” Mon. Not. Roy. Astron. Soc. **504**, 4716–4729 (2021), [Erratum: Mon.Not.Roy.Astron.Soc. 529, 2539–2542 (2024)], arXiv:2102.08382 [astro-ph.CO].
- [92] Jacob Kennedy, Jonathan Colaço Carr, Samuel Gagnon-Hartman, Adrian Liu, Jordan Mirocha, and Yue Cui, “Machine-learning recovery of foreground wedge-removed 21-cm light cones for high-z galaxy mapping,” Mon. Not. Roy. Astron. Soc. **529**, 3684–3698 (2024), arXiv:2308.09740 [astro-ph.CO].

- [93] Nashwan Sabti, Ram Purandhar Reddy Sudha, Julian B. Muñoz, Siddharth Mishra-Sharma, and Tae-wook Youn, “A generative modeling approach to reconstructing 21 cm tomographic data,” *Mach. Learn. Sci. Tech.* **6**, 015039 (2025), arXiv:2407.21097 [astro-ph.CO].
- [94] Emilie Thélie, Franco Del Balso, Julian B. Muñoz, and Adrian Liu, “Alcock-Paczyński test on reionization bubbles for cosmology,” *Phys. Rev. D* **111**, 123501 (2025), arXiv:2502.02638 [astro-ph.CO].
- [95] Matthew McQuinn and Anson D’Aloisio, “The observable 21cm signal from reionization may be perturbative,” *JCAP* **10**, 016 (2018), arXiv:1806.08372 [astro-ph.CO].
- [96] Wenzer Qin, Katelin Schutz, Aaron Smith, Enrico Garaldi, Rahul Kannan, Tracy R. Slatyer, and Mark Vogelsberger, “Effective bias expansion for 21-cm cosmology in redshift space,” *Phys. Rev. D* **106**, 123506 (2022), arXiv:2205.06270 [astro-ph.CO].
- [97] Wenzer Qin, Katelin Schutz, Olivia Rosenstein, Stephanie O’Neil, and Mark Vogelsberger, “Supersizing hydrodynamical simulations of reionization using perturbative techniques,” (2025), arXiv:2504.02929 [astro-ph.CO].
- [98] D. Spergel, N. Gehrels, C. Baltay, D. Bennett, J. Breckinridge, M. Donahue, A. Dressler, B. S. Gaudi, T. Greene, O. Guyon, C. Hirata, J. Kalirai, N. J. Kasdin, B. Macintosh, W. Moos, S. Perlmutter, M. Postman, B. Rauscher, J. Rhodes, Y. Wang, D. Weinberg, D. Benford, M. Hudson, W. S. Jeong, Y. Mellier, W. Traub, T. Yamada, P. Capak, J. Colbert, D. Masters, M. Penny, D. Savransky, D. Stern, N. Zimmerman, R. Barry, L. Bartusek, K. Carpenter, E. Cheng, D. Content, F. Dekens, R. Demers, K. Grady, C. Jackson, G. Kuan, J. Kruk, M. Melton, B. Nemati, B. Parvin, I. Poberezhskiy, C. Peddie, J. Ruffa, J. K. Wallace, A. Whipple, E. Wollack, and F. Zhao, “Wide-Field InfrarRed Survey Telescope–Astrophysics Focused Telescope Assets WFIRST-AFTA 2015 Report,” *arXiv e-prints*, arXiv:1503.03757 (2015), arXiv:1503.03757 [astro-ph.IM].
- [99] N. Aghanim *et al.* (Planck), “Planck 2018 results. VI. Cosmological parameters,” *Astron. Astrophys.* **641**, A6 (2020), [Erratum: *Astron. Astrophys.* 652, C4 (2021)], arXiv:1807.06209 [astro-ph.CO].
- [100] Yu Feng, Uros Seljak, and Matias Zaldarriaga, “Exploring the posterior surface of the large scale structure reconstruction,” *JCAP* **07**, 043 (2018), arXiv:1804.09687 [astro-ph.CO].
- [101] Uriel Frisch, Sabino Matarrese, Roya Mohayaee, and Andrei Sibolevski, “A Reconstruction of the initial conditions of the universe by optimal mass transportation,” *Nature* **417**, 260–262 (2002), arXiv:astro-ph/0109483.
- [102] Y. Brenier, U. Frisch, M. Henon, G. Looper, S. Matarrese, R. Mohayaee, and A. Sobolevskii, “Reconstruction of the early universe as a convex optimization problem,” *Mon. Not. Roy. Astron. Soc.* **346**, 501–524 (2003), arXiv:astro-ph/0304214.
- [103] Daniel J. Eisenstein, Hee-jong Seo, Edwin Sirk, and David Spergel, “Improving Cosmological Distance Measurements by Reconstruction of the Baryon Acoustic Peak,” *Astrophys. J.* **664**, 675–679 (2007), arXiv:astro-ph/0604362.
- [104] Jens Jasche and Benjamin D. Wandelt, “Bayesian physical reconstruction of initial conditions from large scale structure surveys,” *Mon. Not. Roy. Astron. Soc.* **432**, 894 (2013), arXiv:1203.3639 [astro-ph.CO].
- [105] Francisco-Shu Kitaura, “The Initial Conditions of the Universe from Constrained Simulations,” *Mon. Not. Roy. Astron. Soc.* **429**, 84 (2013), arXiv:1203.4184 [astro-ph.CO].
- [106] Svetlin Tassev and Matias Zaldarriaga, “Towards an Optimal Reconstruction of Baryon Oscillations,” *JCAP* **10**, 006 (2012), arXiv:1203.6066 [astro-ph.CO].
- [107] Huiyuan Wang, H. J. Mo, Xiaohu Yang, and Frank C. van den Bosch, “Reconstructing the Initial Density Field of the Local Universe: Methods and Tests with Mock Catalogs,” *Astrophys. J.* **772**, 63 (2013), arXiv:1301.1348 [astro-ph.CO].
- [108] Marcel Schmittfull, Tobias Baldauf, and Matias Zaldarriaga, “Iterative initial condition reconstruction,” *Phys. Rev. D* **96**, 023505 (2017), arXiv:1704.06634 [astro-ph.CO].
- [109] Uros Seljak, Grigor Aslanyan, Yu Feng, and Chirag Modi, “Towards optimal extraction of cosmological information from nonlinear data,” *JCAP* **12**, 009 (2017), arXiv:1706.06645 [astro-ph.CO].
- [110] Ryuichiro Hada and Daniel J. Eisenstein, “An iterative reconstruction of cosmological initial density fields,” *Mon. Not. Roy. Astron. Soc.* **478**, 1866–1874 (2018), arXiv:1804.04738 [astro-ph.CO].
- [111] Chirag Modi, Yu Feng, and Uros Seljak, “Cosmological Reconstruction From Galaxy Light: Neural Network Based Light-Matter Connection,” *JCAP* **10**, 028 (2018), arXiv:1805.02247 [astro-ph.CO].
- [112] Yu Liu, Yu Yu, and Baojiu Li, “Biased Tracer Reconstruction with Halo Mass Information,” *Astrophys. J. Suppl.* **254**, 4 (2021), arXiv:2012.11251 [astro-ph.CO].
- [113] Xinyi Chen and Nikhil Padmanabhan, “Analysis of an iterative reconstruction method in comparison of the standard reconstruction method,” *Mon. Not. Roy. Astron. Soc.* **534**, 1490–1503 (2024), arXiv:2311.09531 [astro-ph.CO].
- [114] Chirag Modi, Martin White, Anze Slosar, and Emanuele Castorina, “Reconstructing large-scale structure with neutral hydrogen surveys,” *JCAP* **11**, 023 (2019), arXiv:1907.02330 [astro-ph.CO].
- [115] Meng Zhou and Yi Mao, “Reconstruction of Cosmological Initial Density Field with Observations from the Epoch of Reionization,” *Astrophys. J.* **965**, 31 (2024), arXiv:2311.14940 [astro-ph.CO].
- [116] Shu-Fan Chen, Kai-Feng Chen, and Cora Dvorkin, “Field-level Reconstruction from Foreground-Contaminated 21-cm Maps,” (in preparation).
- [117] David W. Hogg, “Distance measures in cosmology,” *arXiv e-prints*, astro-ph/9905116 (1999), arXiv:astro-ph/9905116 [astro-ph].
- [118] Steven G. Murray and C. M. Trott, “The Effect of Baseline Layouts on the Epoch of Reionization Foreground Wedge: A Semianalytical Approach,” *ApJ* **869**, 25 (2018), arXiv:1810.10712 [astro-ph.IM].
- [119] Vincent MacKay, Zhilei Xu, Ruby Byrne, and Jacqueline Hewitt, “The RULES Algorithm to Generate Realistic *uv*-Complete Radio Arrays, with Application to 21 cm Foreground Wedge Removal,” (in preparation).
- [120] M. H. Goroff, Benjamin Grinstein, S. J. Rey, and Mark B. Wise, “Coupling of Modes of Cosmological Mass Density Fluctuations,” *Astrophys. J.* **311**, 6–14 (1986).

- [121] Bhuvnesh Jain and Edmund Bertschinger, “Second order power spectrum and nonlinear evolution at high redshift,” *Astrophys. J.* **431**, 495 (1994), [arXiv:astro-ph/9311070](#).
- [122] F. Bernardeau, S. Colombi, E. Gaztanaga, and R. Scoccimarro, “Large scale structure of the universe and cosmological perturbation theory,” *Phys. Rept.* **367**, 1–248 (2002), [arXiv:astro-ph/0112551](#).
- [123] Tobias Baldauf, Lorenzo Mercolli, Mehrdad Mirbabayi, and Enrico Pajer, “The Bispectrum in the Effective Field Theory of Large Scale Structure,” *JCAP* **05**, 007 (2015), [arXiv:1406.4135 \[astro-ph.CO\]](#).
- [124] Valentin Assassi, Daniel Baumann, Daniel Green, and Matias Zaldarriaga, “Renormalized Halo Bias,” *JCAP* **08**, 056 (2014), [arXiv:1402.5916 \[astro-ph.CO\]](#).
- [125] Chung-Pei Ma and Edmund Bertschinger, “Cosmological perturbation theory in the synchronous and conformal Newtonian gauges,” *Astrophys. J.* **455**, 7–25 (1995), [arXiv:astro-ph/9506072](#).
- [126] Antony Lewis, Anthony Challinor, and Anthony Lasenby, “Efficient computation of CMB anisotropies in closed FRW models,” *ApJ* **538**, 473–476 (2000), [arXiv:astro-ph/9911177 \[astro-ph\]](#).
- [127] Julien Lesgourgues, “The cosmic linear anisotropy solving system (class) i: Overview,” arXiv preprint [arXiv:1104.2932](#) (2011).
- [128] Andrei Mesinger, Steven Furlanetto, and Renyue Cen, “21CMFAST: a fast, seminumerical simulation of the high-redshift 21-cm signal,” *MNRAS* **411**, 955–972 (2011), [arXiv:1003.3878 \[astro-ph.CO\]](#).
- [129] Steven Murray, Bradley Greig, Andrei Mesinger, Julian Muñoz, Yuxiang Qin, Jaehong Park, and Catherine Watkinson, “21cmFAST v3: A Python-integrated C code for generating 3D realizations of the cosmic 21cm signal,” *The Journal of Open Source Software* **5**, 2582 (2020), [arXiv:2010.15121 \[astro-ph.IM\]](#).
- [130] Steven R. Furlanetto, Matias Zaldarriaga, and Lars Hernquist, “The Growth of H II Regions During Reionization,” *ApJ* **613**, 1–15 (2004), [arXiv:astro-ph/0403697 \[astro-ph\]](#).
- [131] Jaehong Park, Andrei Mesinger, Bradley Greig, and Nicolas Gillet, “Inferring the astrophysics of reionization and cosmic dawn from galaxy luminosity functions and the 21-cm signal,” *MNRAS* **484**, 933–949 (2019), [arXiv:1809.08995 \[astro-ph.GA\]](#).
- [132] Julian B. Muñoz, “An effective model for the cosmic-dawn 21-cm signal,” *Mon. Not. Roy. Astron. Soc.* **523**, 2587–2607 (2023), [arXiv:2302.08506 \[astro-ph.CO\]](#).
- [133] Antony Lewis and Anthony Challinor, “CAMB: Code for Anisotropies in the Microwave Background,” *Astrophysics Source Code Library*, record ascl:1102.026 (2011).
- [134] R. J. Bouwens, G. D. Illingworth, P. A. Oesch, M. Trenti, I. Labb  , L. Bradley, M. Carollo, P. G. van Dokkum, V. Gonzalez, B. Holwerda, M. Franx, L. Spitler, R. Smit, and D. Magee, “UV Luminosity Functions at Redshifts $z \sim 4$ to $z \sim 10$: 10,000 Galaxies from HST Legacy Fields,” *ApJ* **803**, 34 (2015), [arXiv:1403.4295 \[astro-ph.CO\]](#).
- [135] Steven L. Finkelstein, Russell E. Ryan, Jr., Casey Papovich, Mark Dickinson, Mimi Song, Rachel S. Somerville, Henry C. Ferguson, Brett Salmon, Mauro Giavalisco, Anton M. Koekemoer, Matthew L. N. Ashby, Peter Behroozi, Marco Castellano, James S. Dunlop, Sandy M. Faber, Giovanni G. Fazio, Adriano Fontana, Norman A. Grogin, Nimish Hathi, Jason Jaacks, Dale D. Kocevski, Rachael Livermore, Ross J. McLure, Emiliano Merlin, Bahram Mobasher, Jeffrey A. Newman, Marc Rafelski, Vithal Tilvi, and S. P. Willner, “The Evolution of the Galaxy Rest-frame Ultraviolet Luminosity Function over the First Two Billion Years,” *ApJ* **810**, 71 (2015), [arXiv:1410.5439 \[astro-ph.GA\]](#).
- [136] Micaela B. Bagley, Claudia Scarlata, Alaina Henry, Marc Rafelski, Matthew Malkan, Harry Teplitz, Y. Sophia Dai, Ivano Baronchelli, James Colbert, Michael Rutkowski, Vihang Mehta, Alan Dressler, Patrick McCarthy, Andrew Bunker, Hakim Atek, Thibault Garel, Crystal L. Martin, Nimish Hathi, and Brian Siana, “A High Space Density of Luminous Lyman Alpha Emitters at $z \sim 6.5$,” *ApJ* **837**, 11 (2017), [arXiv:1701.05193 \[astro-ph.CO\]](#).
- [137] Marcia J. Rieke, Brant Robertson, Sandro Tacchella, Kevin Hainline, Benjamin D. Johnson, Ryan Hausen, Zhiyuan Ji, Christopher N. A. Willmer, Daniel J. Eisenstein, D  vid Pusk  s, Stacey Alberts, Santiago Arribas, William M. Baker, Stefi Baum, Rachana Bhatawdekar, Nina Bonaventura, Kristan Boyett, Andrew J. Bunker, Alex J. Cameron, Stefano Carniani, Stephane Charlot, Jacopo Chevallard, Zuyi Chen, Mirko Curti, Emma Curtis-Lake, A. Lola Danhaive, Christa DeCoursey, Alan Dressler, Eiichi Egami, Ryan Endsley, Jakob M. Helton, Raphael E. Hviding, Nimisha Kumari, Tobias J. Looser, Jianwei Lyu, Roberto Maiolino, Michael V. Maseda, Erica J. Nelson, George Rieke, Hans-Walter Rix, Lester Sandles, Aayush Saxena, Katherine Sharpe, Irene Shavaei, Maya Skarbinski, Renske Smit, Daniel P. Stark, Meredith Stone, Katherine A. Suess, Fengwu Sun, Michael Topping, Hannah   bler, Natalia C. Vilanueva, Imaan E. B. Wallace, Christina C. Williams, Chris Willott, Lily Whitler, Joris Witstok, and Charity Woodrum, “JADES Initial Data Release for the Hubble Ultra Deep Field: Revealing the Faint Infrared Sky with Deep JWST NIRCam Imaging,” *ApJS* **269**, 16 (2023), [arXiv:2306.02466 \[astro-ph.GA\]](#).
- [138] Pablo Arrabal Haro, Mark Dickinson, Steven L. Finkelstein, Seiji Fujimoto, Vital Fern  ndez, Jeyhan S. Kartaltepe, Intae Jung, Justin W. Cole, Denis Burgarella, Katherine Chworowsky, Taylor A. Hutchison, Alexa M. Morales, Casey Papovich, Raymond C. Simons, Ricardo O. Amor  n, Bren E. Backhaus, Micaela B. Bagley, Laura Bisigello, Antonello Calab  r, Marco Castellano, Nikko J. Cleri, Romeel Dav  , Avishai Dekel, Henry C. Ferguson, Adriano Fontana, Eric Gawiser, Mauro Giavalisco, Santosh Harish, Nimish P. Hathi, Michaela Hirschmann, Benne W. Holwerda, Marc Huertas-Company, Anton M. Koekemoer, Rebecca L. Larson, Ray A. Lucas, Bahram Mobasher, Pablo G. P  rez-Gonz  lez, Nor Pirzkal, Caitlin Rose, Paola Santini, Jonathan R. Trump, Alexander de la Vega, Xin Wang, Benjamin J. Weiner, Stephen M. Wilkins, Guang Yang, L. Y. Aaron Yung, and Jorge A. Zavala, “Spectroscopic Confirmation of CEERS NIRCam-selected Galaxies at $z \simeq 8\text{--}10$,” *ApJ* **951**, L22 (2023), [arXiv:2304.05378 \[astro-ph.GA\]](#).
- [139] Steven L. Finkelstein, “Observational Searches for Star-Forming Galaxies at $z > 6$,” *PASA* **33**, e037 (2016), [arXiv:1511.05558 \[astro-ph.GA\]](#).

- [140] Zhen-Ya Zheng, Junxian Wang, James Rhoads, Leopoldo Infante, Sangeeta Malhotra, Weida Hu, Alastair R. Walker, Linhua Jiang, Chunyan Jiang, Pascale Hibon, Alicia Gonzalez, Xu Kong, XianZhong Zheng, Gaspar Galaz, and L. Felipe Barrientos, “First Results from the Lyman Alpha Galaxies in the Epoch of Reionization (LAGER) Survey: Cosmological Reionization at $z \sim 7$,” *ApJ* **842**, L22 (2017), arXiv:1703.02985 [astro-ph.GA].
- [141] Satoshi Kikuta, Masami Ouchi, Takatoshi Shibuya, Yongming Liang, Hiroya Umeda, Akinori Matsumoto, Kazuhiro Shimasaku, Yuichi Harikane, Yoshiaki Ono, Akio K. Inoue, Satoshi Yamanaka, Haruka Kusakabe, Rieko Momose, Nobunari Kashikawa, Yuichi Matsuda, and Chien-Hsiu Lee, “SILVERRUSH. XIII. A Catalog of 20,567 Ly α Emitters at $z = 2\text{--}7$ Identified in the Full-depth Data of the Subaru/HSC-SSP and CHORUS Surveys,” *ApJS* **268**, 24 (2023), arXiv:2305.08921 [astro-ph.GA].
- [142] Roman Observations Time Allocation Committee and Core Community Survey Definition Committees, “Roman Observations Time Allocation Committee: Final Report and Recommendations,” arXiv e-prints, arXiv:2505.10574 (2025), arXiv:2505.10574 [astro-ph.IM].
- [143] Charles R. Harris *et al.*, “Array programming with NumPy,” *Nature* **585**, 357–362 (2020), arXiv:2006.10256 [cs.MS].
- [144] Pauli Virtanen, Ralf Gommers, Travis E. Oliphant, Matt Haberland, Tyler Reddy, David Cournapeau, Evgeni Burovski, Pearu Peterson, Warren Weckesser, Jonathan Bright, Stéfan J. van der Walt, Matthew Brett, Joshua Wilson, K. Jarrod Millman, Nikolay Mayorov, Andrew R. J. Nelson, Eric Jones, Robert Kern, Eric Larson, C. J. Carey, İlhan Polat, Yu Feng, Eric W. Moore, Jake VanderPlas, Denis Laxalde, Josef Perktold, Robert Cimrman, Ian Henriksen, E. A. Quintero, Charles R. Harris, Anne M. Archibald, Antônio H. Ribeiro, Fabian Pedregosa, Paul van Mulbregt, and SciPy 1.0 Contributors, “SciPy 1.0: fundamental algorithms for scientific computing in Python,” *Nature Methods* **17**, 261–272 (2020), arXiv:1907.10121 [cs.MS].
- [145] Thomas Kluyver *et al.*, “Jupyter notebooks - a publishing format for reproducible computational workflows,” in *ELPUB* (2016).
- [146] Casper O. da Costa-Luis, “tqdm: A fast, extensible progress meter for python and cli,” *Journal of Open Source Software* **4**, 1277 (2019).
- [147] John D. Hunter, “Matplotlib: A 2D Graphics Environment,” *Comput. Sci. Eng.* **9**, 90–95 (2007).